Materials for Advanced Ultrasupercritical Steam Turbines

Topical Report
Task 3: Materials for Non-Welded Rotors, Buckets, and Bolting
Oct. 1, 2009 – Sept. 30, 2015

Submitted To:
Energy Industries of Ohio

Author:
Deepak Saha

Submitted By:
GE Power and Water
Schenectady, NY 12345

September 2015

DOE Cooperative Agreement No. DE-FE0000234

DISCLAIMER

ABSTRACT

The primary objective of the task was to characterize the materials suitable for mechanically coupled rotor, buckets and bolting operating with an inlet temperature of 760°C (1400°F). A previous study DOE-FC26-05NT42442, identified alloys such as Haynes®282®, Nimonic 105, Inconel 740, Waspaloy, Nimonic 263, and Inconel 617 as potential alloys that met the requirements for the necessary operating conditions. Of all the identified materials, Waspaloy has been widely utilized in the aviation industry in the form of disk and other smaller forgings, and sufficient material properties and vendor experience exist, for the design and manufacture of large components. The European program characterizing materials for A-USC conditions are evaluating Nimonic 263 and Inconel 617 for large components. Inconel 740 has been studied extensively as a part of the boiler consortium and is code approved. Therefore, the consortium focused efforts in the development of material properties for Haynes®282® and Nimonic 105 to avoid replicative efforts and provide material choices/trade off during the detailed design of large components.

Commercially available Nimonic 105 and Haynes®282® were evaluated for microstructural stability by long term thermal exposure studies. Material properties requisite for design such as tensile, creep / rupture, low cycle fatigue, high cycle fatigue, fatigue crack growth rate, hold-time fatigue, fracture toughness, and stress relaxation are documented in this report.

A key requisite for the success of the program was a need demonstrate the successful scale up of the down-selected alloys, to large components. All property evaluations in the past were performed on commercially available bar/billet forms. Components in power plant equipment such as rotors and castings are several orders in magnitude larger and there is a real need to resolve the scalability issue. Nimonic 105 contains high volume fraction γ' [>50%], and hence the alloy is best suited for smaller forging and valve internals, bolts, smaller blades. Larger Nimonic 105 forgings, would precipitate γ' during the surface cooling during forging, leading to surface cracks. The associate costs in forging Nimonic 105 to larger sizes [hotter dies, press requirements], were beyond the scope of this task and not investigated further. Haynes®282® has 20 - 25% volume fraction γ' was a choice for large components, albeit untested.

A larger ingot diameter is pre-requisite for a larger diameter forging and achieves the "typically" accepted working ratio of 2.5-3:1. However, Haynes®282® is manufactured via a double melt process [VIM-ESR] limited by size [<18-16" diameter], which limited the maximum size of the final forging. The report documents the development of a 24" diameter triple melt ingot, surpassing the current available technology. A second triple melt ingot was manufactured and successfully forged into a 44" diameter disk. The successful developments in triple melting process and the large diameter forging of Haynes®282® resolved the scalability issues and involved the first of its kind attempt in the world for this alloy. The complete characterization of Haynes®282® forging was performed and documented in this report. The dataset from the commercially available Haynes®282® [grain size ASTM 3-4] and the finer grain size disk forging [ASTM 8-9] offer an additional design tradeoff to balance creep and fatigue during the future design process.

TABLE OF CONTENTS

FIGURES

TABLES

LIST OF ACRONYMS AND ABBREVIATIONS

TEM……	Transmission Electron Microscope
γ'……..	Gamma Prime
UTS……	Ultimate Tensile Strength
0.2YS……	0.2% Yield Strength
% Elongation……	% Elongation to failure
%RA……...	% Reduction in Area
LMP……	Larson-Miller Parameter
KQ……..	Conditional Fracture Toughness
VIM……	Vacuum Induction Melting
ESR……	Electrode Slag Remelting
VAR……	Vacuum Arc Remelting

PROJECT BACKGROUND & INTRODUCTION

The overall objective of the project is to contribute to the development of materials technology for use in advanced ultrasupercritical (A-USC) pulverized coal power plants capable of operating with steam up to 760°C (1400°F), 35 MPa (5000 psi). R&D is needed on newly developed materials to lead to a full-scale demonstration, and eventual commercialization, of A-USC power plants. The lack of materials with the necessary fabricability and resistance to creep, oxidation, corrosion and fatigue at the higher steam temperatures and pressures currently limit the adoption of A-USC steam conditions in pulverized coal-fired plants.

A Phase 1 (three year national effort) sponsored by the U.S. Department of Energy (DOE) and the Ohio Coal Development Office (OCDO) was completed in June 2009 and the final report was submitted. The Phase 1 effort was performed under a prime contract with Energy Industries of Ohio (EIO) through a consortium made up of the Electric Power Research Institute (EPRI), Oak Ridge National Laboratory (ORNL) and all of the U.S. domestic turbine manufactures: General Electric, Alstom Power and Siemens Westinghouse. This initial Phase 1 addressed the need to identify and analyze candidate USC turbine materials from the perspective of steam side conditions and pressure ranges to be encountered in A-USC turbines. The Phase 1 effort has accomplished these goals, and a more robust five year Phase 2 effort has just been initiated. This Phase 2 efforts focused on the identified candidate alloys to address specific fabrication abilities, particularly metal casting, of these alloys for use in making components such as casings, housings, valves and ingots. In particular, efforts associated with high nickel alloys will be targeted for developing the specific means of casting these alloys using electric arc AOD (argon-oxygen-decarburization), vacuum and/or pressure casting.

At the completion of Phase 1, Alstom Power and Siemens Corporation withdrew participation due to business reasons. Funding for Phase 2 is now being provided by OCDO and DOE with cost sharing and technical participation from General Electric, Co. and EPRI. Oak Ridge National Laboratory and NETL-Albany Research Center are also participating in the project and are being funded directly by DOE to provide support.

Specific objectives of the Phase 2 effort include conducting more detailed evaluations of the weldability, mechanical properties and reparability of the selected candidate alloys for rotors, casings and valves and to perform scale up studies to establish a design basis for commercial scale components. A supplemental program funded by the OCDO will undertake supporting tasks such as testing and trials using existing atmospheric, vacuum and developmental pressure furnaces to define specific metal casting techniques needed for producing commercial scale components.

The goal of this task was to continue to develop and assess materials for non-welded rotors, buckets and bolting for the steam turbine. Two potential alloys were considered in Phase 1 of this project and documented in report DE-FC26-05NT42445. The potential alloys that met the requisite creep rupture properties were identified as Nimonic 105 and

Haynes 282 (primarily based on creep rupture life of 250,000 hours at 15 Ksi) and LCF life. The primary goal of Phase 2 is twofold;

1) Develop sufficient mechanical property information on nickel-base blade/bolting candidate alloys so preliminary steam turbine design calculations for rotors, buckets and bolts and valve internals can be initiated

2) Analyze the materials under study:

- Understand the effect of environment on fatigue
- Measure long term mechanical property degradation due to high temperature exposure
- Characterize the micro-structure
- Determine strengthening precipitate coarsening behavior
- Identify any deleterious phases that might degrade long term properties

EVALUATION OF NIMONIC 105

Phase 1 of the program [DOE-FC26-05NT42442] characterized material of Nimonic 105 obtained from 2" diameter bar. In this program 8.75" diameter hot finished billet for testing. The material was heat treated to achieve peak hardness

Solution Anneal:	2100°F (1149°C)	4 Hours
Age Treatment 1:	1950°F (1066°C)	16 Hours
Age Treatment 2:	1560°F (849°C)	16 Hours

The billet was cut into two additional pieces and placed in a furnace maintained at 1425°F (774°C). The two pieces would provide data on the embrittlement of the material during the long term exposure of this alloy. The National Energy Technology Laboratory (NETL) provided the transmission electron microscope (TEM) analysis of the 2" diameter Nimonic alloy. The primary γ' size was estimated to be in the range of 60 nm [Figure 1].

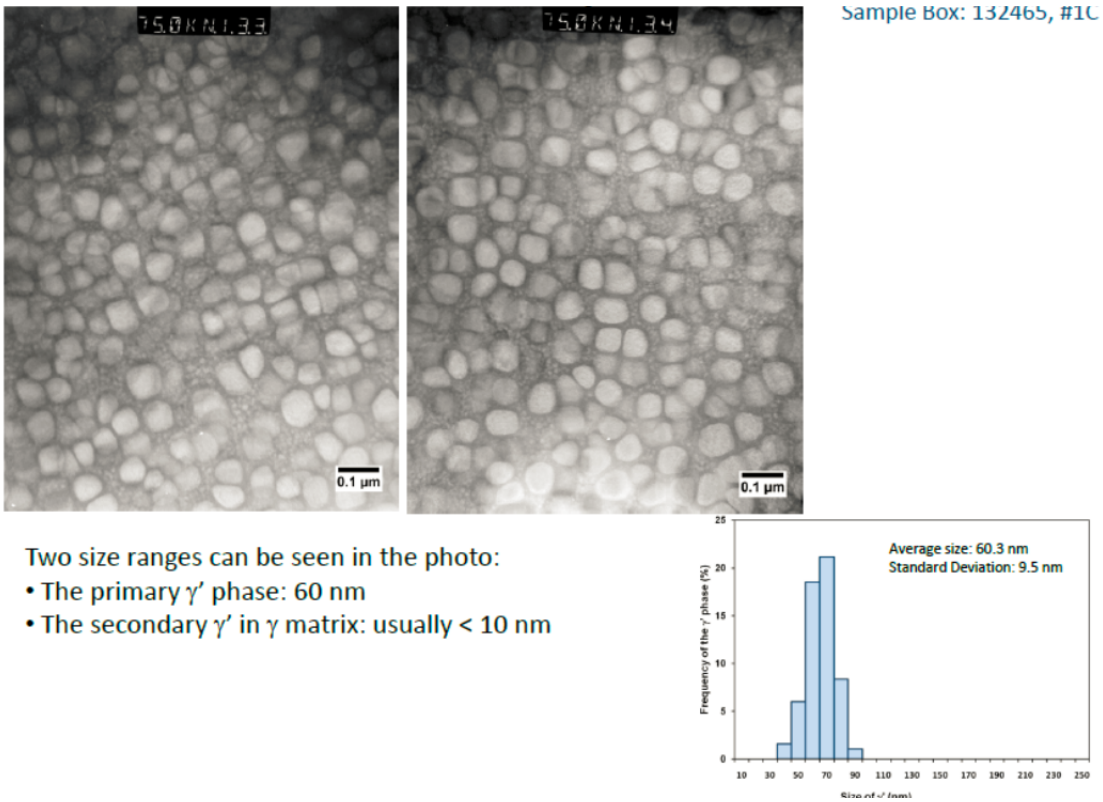

Figure 1: Typical γ' precipitate size in Nimonic 105

Similar TEM analysis was performed by GE Global Research on the starting γ' form the 8.75" diameter billet. The size was double the smaller diameter bar and in the range of

140-150 nm [Figure 2]. Figure 3 shows the presence of $Cr_{23}C_6$ as primary carbide phase in N105 at the grain boundary of Nimonic 105.

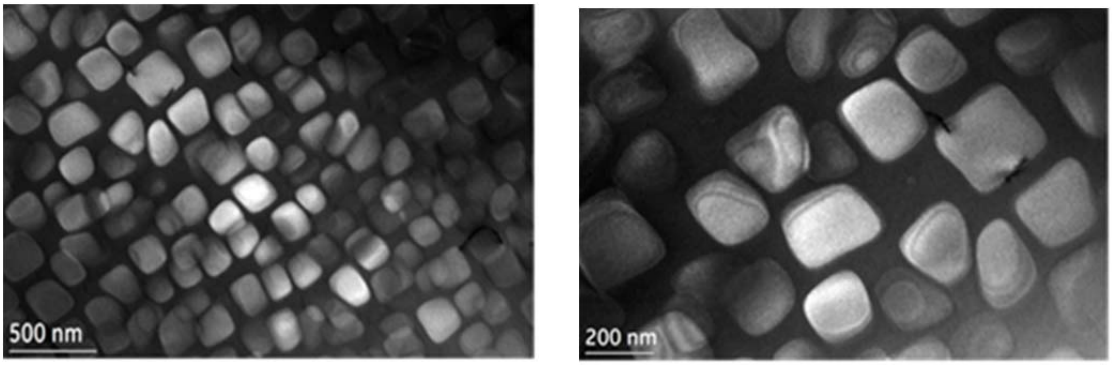

Figure 2 Typical γ' precipitate size in Nimonic 105 from 8.75" diameter billet

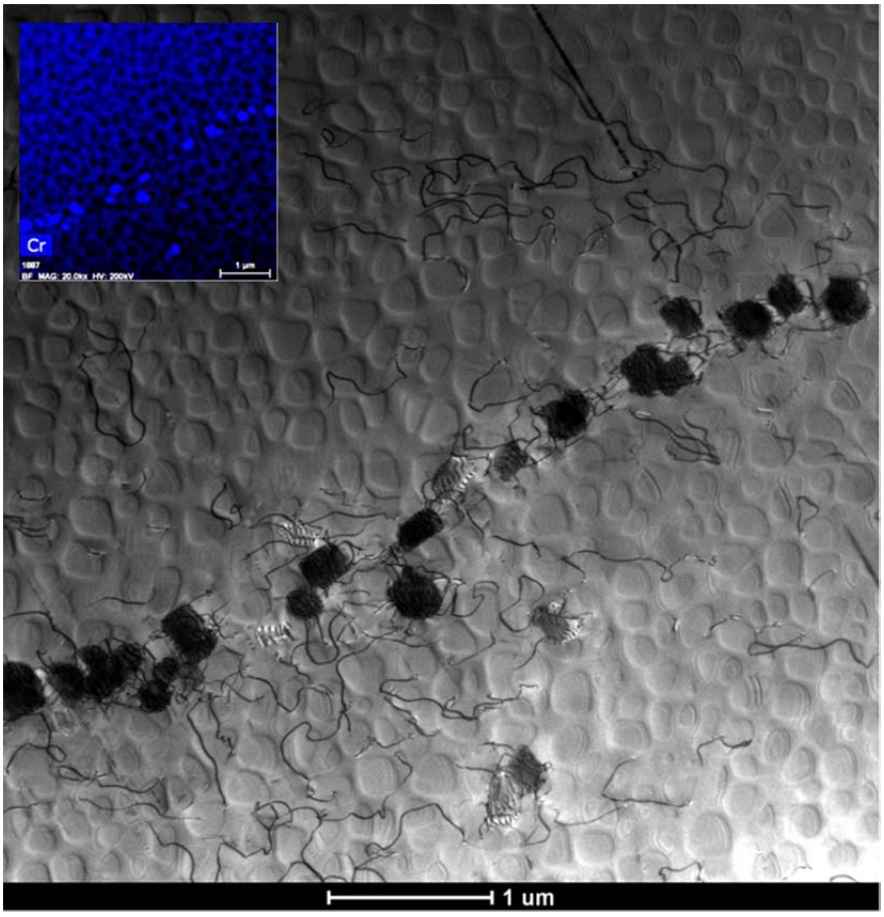

Figure 3: TEM image identifying $Cr_{23}C_6$ as primary carbide phase in N105

Figure 4 through Figure 11 show the properties obtained from Nimonic 105 after a thermal exposure of 1425°F (774°C) for 1 year / 8760 hours and 2 year / 17500 hours. The data consists of a mix of different orientations and is compared against baseline data tests obtained from the Phase 1 report. Based on the dataset Nimonic 105 shows

a debit in Elongation and Reduction of Area (RA) after a year of exposure and levels after the initial drop. This is very typical of Nickel based alloys due to the coarsening of γ'. The longitudinal orientation exhibited % Elongation and % RA in excess of acceptable values of 10%.

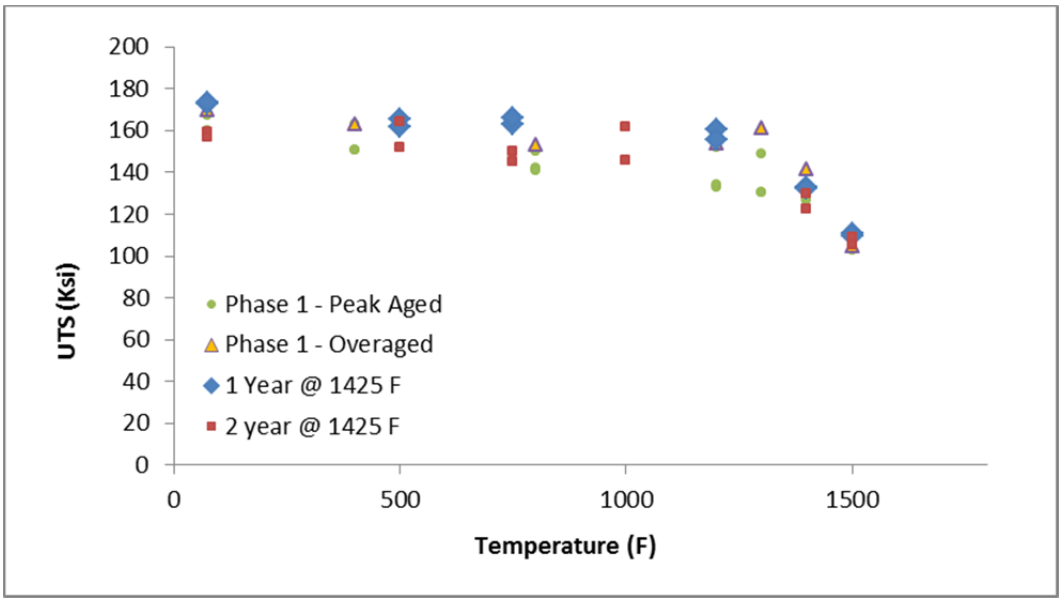

Figure 4: Tensile strength in Nimonic 105 after a 1 & 2 year thermal exposure at 1425°F (774°C) [Longitudinal Orientation]

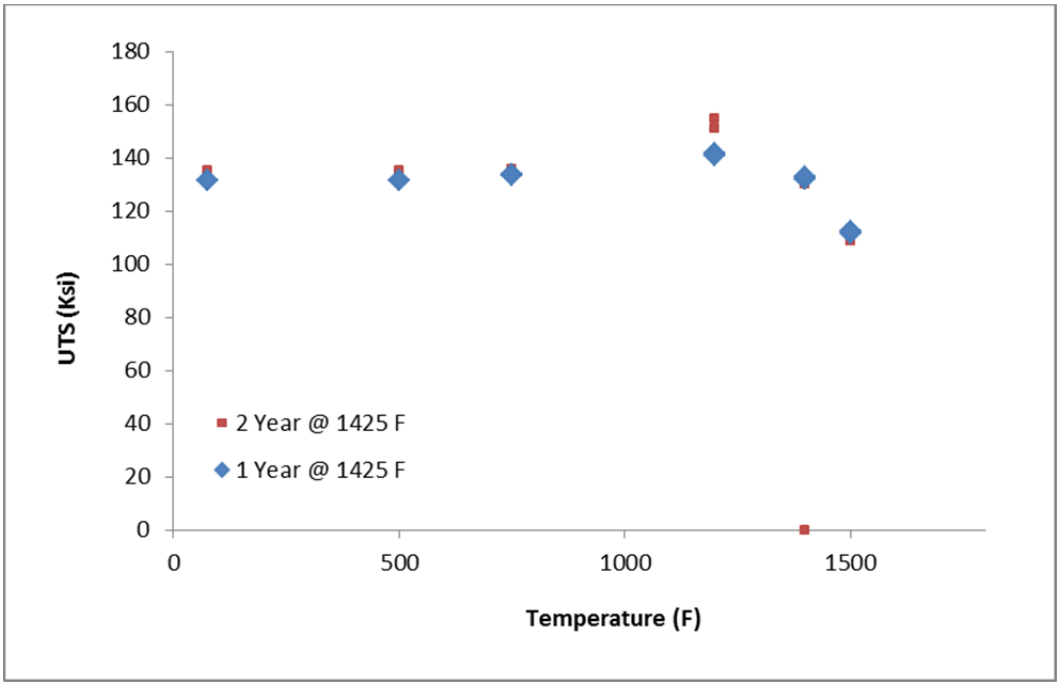

Figure 5: Tensile strength in Nimonic 105 after a 1 & 2 year thermal exposure at 1425°F (774°C) [Transverse Orientation]

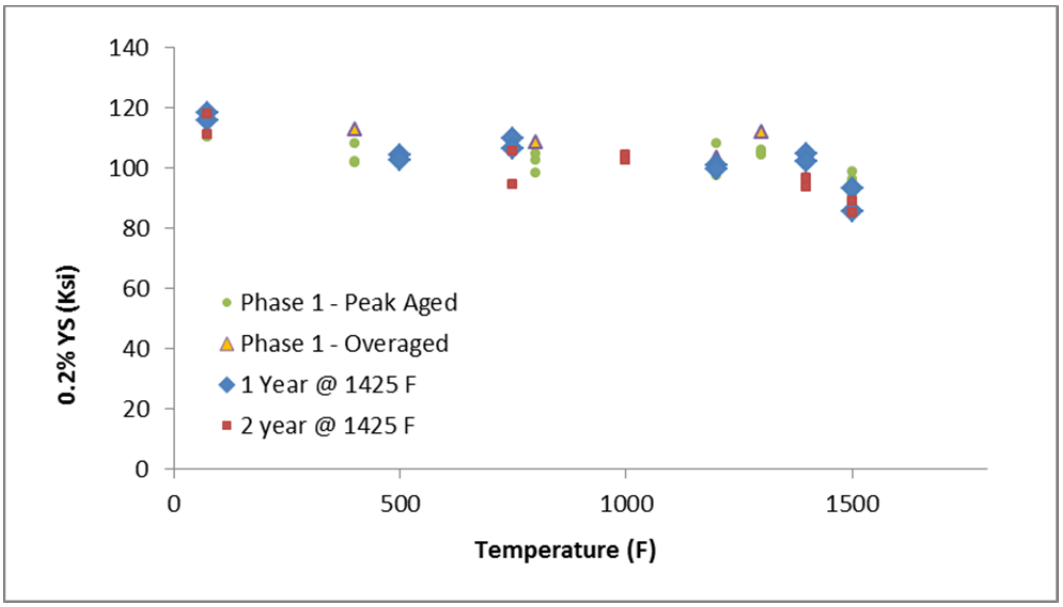

Figure 6: 0.2% Yield Strength in Nimonic 105 after a 1 & 2 year thermal exposure at 1425°F (774°C) *[Longitudinal Orientation]*

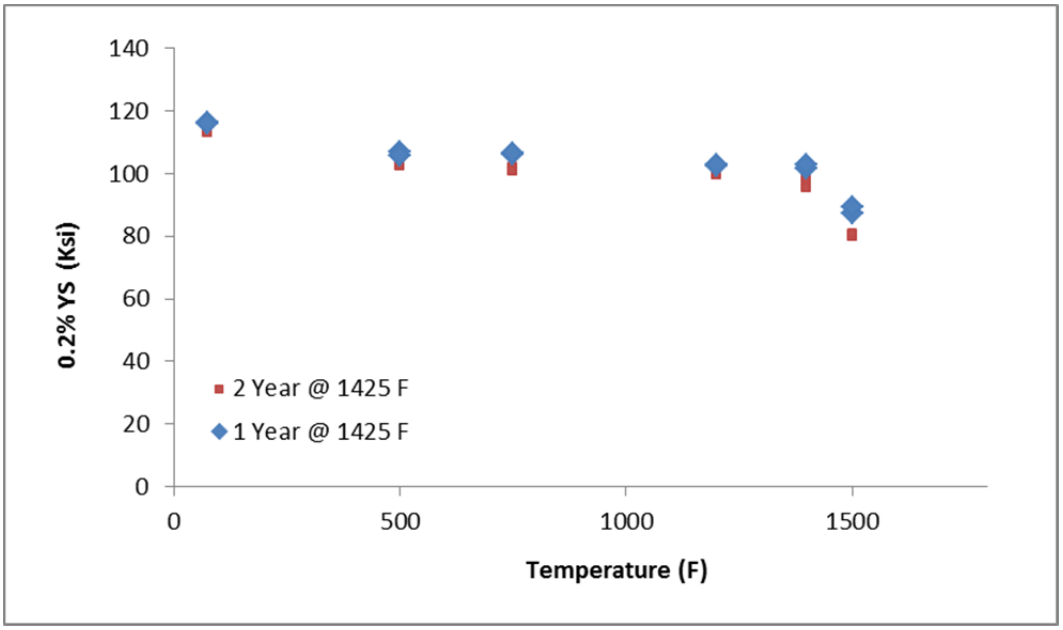

Figure 7: 0.2% Yield Strength in Nimonic 105 after a 1 & 2 year thermal exposure at 1425°F (774°C) [*Transverse Orientation*]

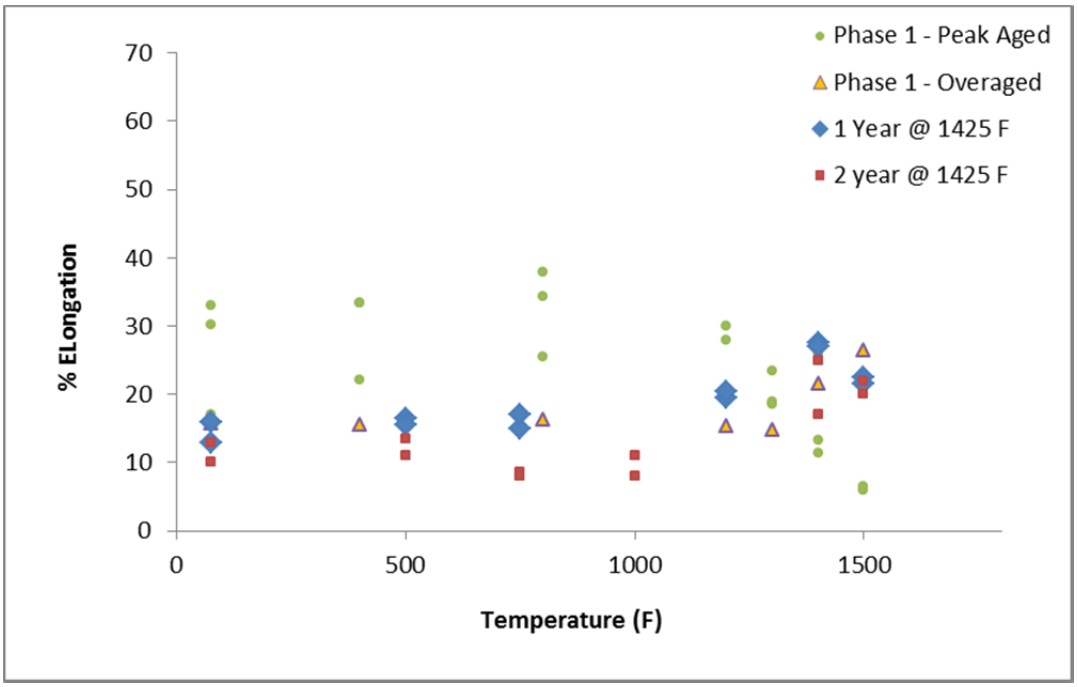

Figure 8: % Elongation in Nimonic 105 after a 1 & 2 year thermal exposure at 1425°F (774°C) [*Longitudinal Orientation*]

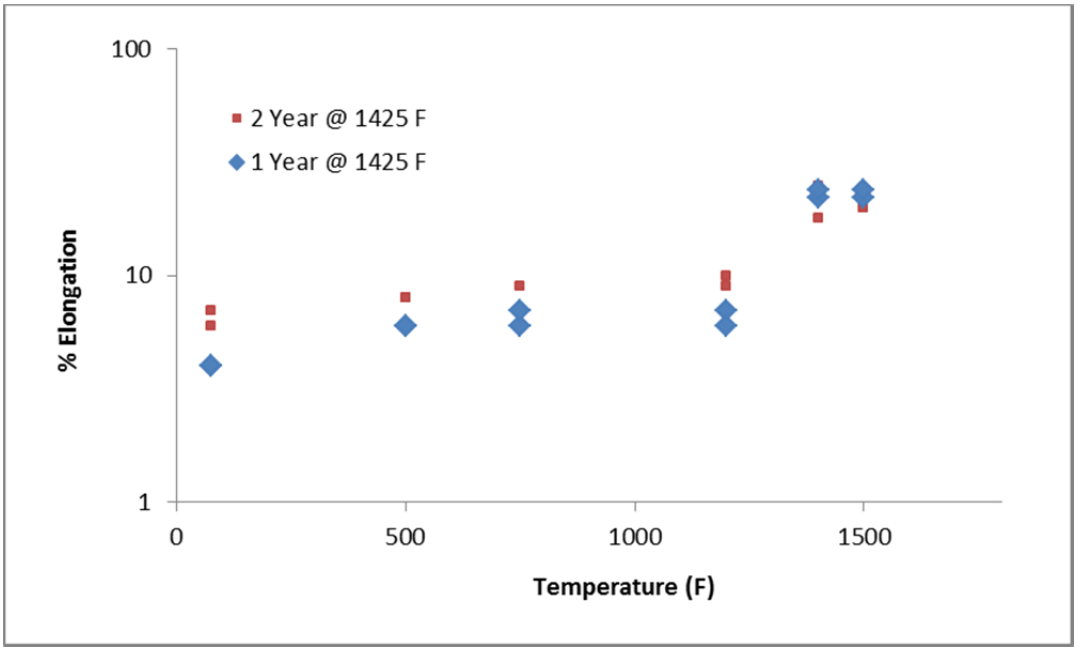

Figure 9: % Elongation in Nimonic 105 after a 1 & 2 year thermal exposure at 1425°F (774°C) [*Transverse Orientation*]

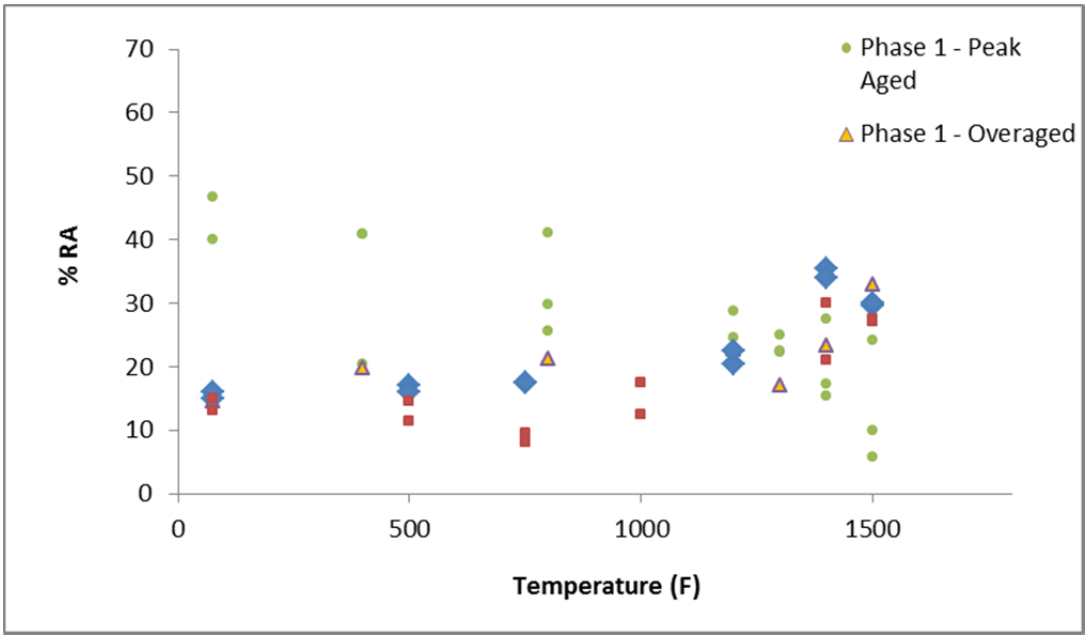

Figure 10: % RA in Nimonic 105 after a 1 & 2 year thermal exposure at 1425°F (774°C) [*Longitudinal Orientation*]

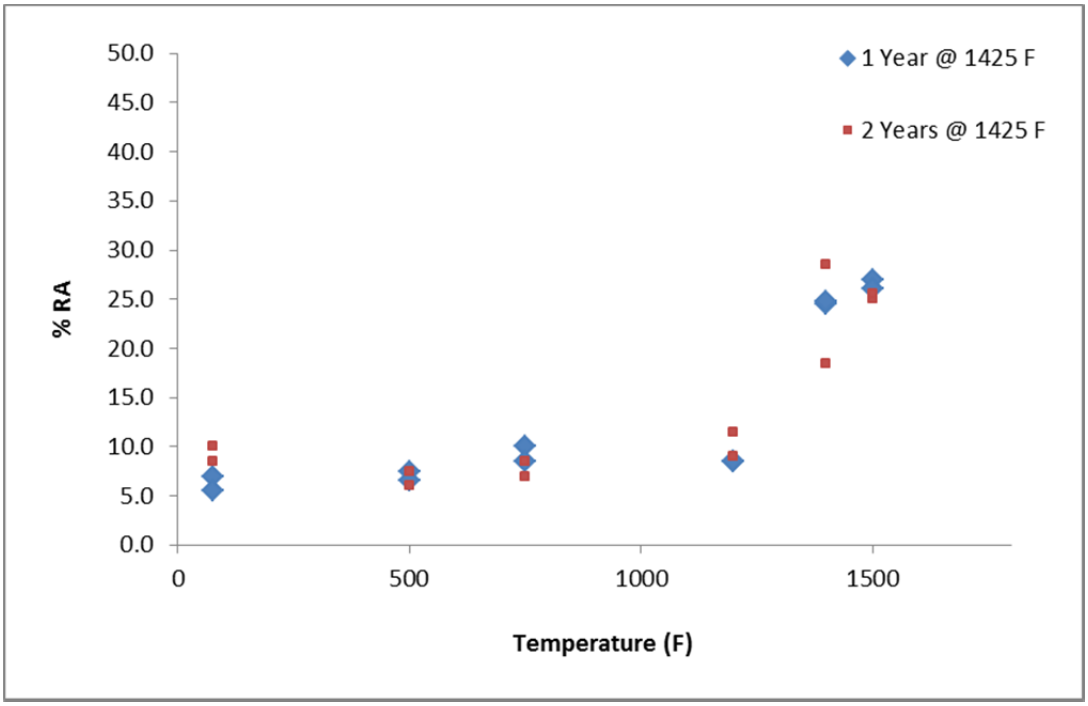

Figure 11: % RA in Nimonic 105 after a 1 & 2 year thermal exposure at 1425°F (774°C) [*Transverse Orientation*]

Multiple specimens were extracted from the bar for fracture toughness testing. The specimens were 0.75" thick [B] and 1.5" Wide [W]. All specimens were side grooved to a depth equal to 20% of the nominal thickness [10% each side]. The specimens were tested in accordance to ASTM E1820-09. As specimens had a mix of valid and invalid

fracture toughness, J1c, Figure 12 plots only the conditional fracture toughness of Nimonic 105 as a function of temperature and thermal exposure. No debit was observed during the thermal exposure of Nimonic 105 over a two year period at 1425°F (774°C).

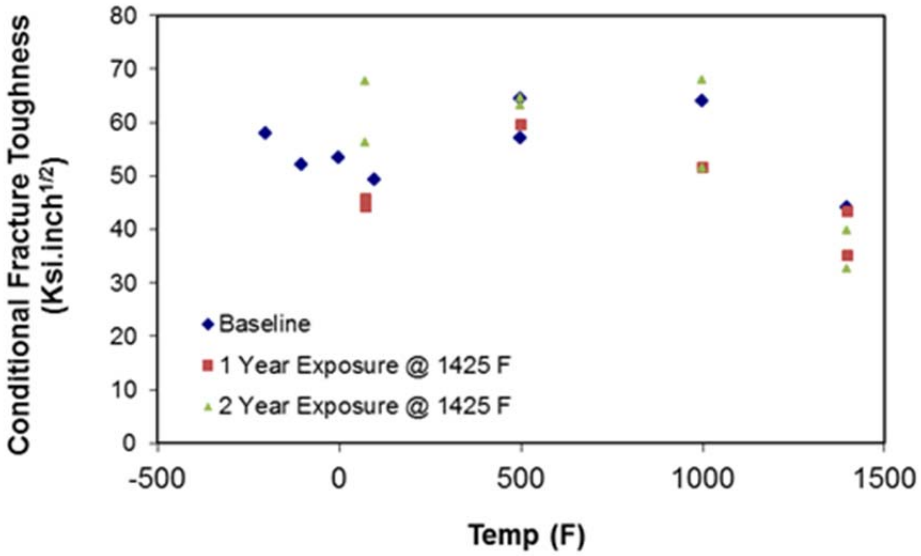

Figure 12: Toughness in Nimonic 105 after a 1 & 2 year thermal exposure at 1425°F (774°C)

Fatigue specimens were machined from the bar [longitudinal orientation only] and subjected to high cycle fatigue tests [in air]. All tests were performed at 1400°F (760°C), 50 Hertz and 10,000,000 cycles runout. Figure 13 shows the plot of alternating stress and cycles to failure for various A ratios.

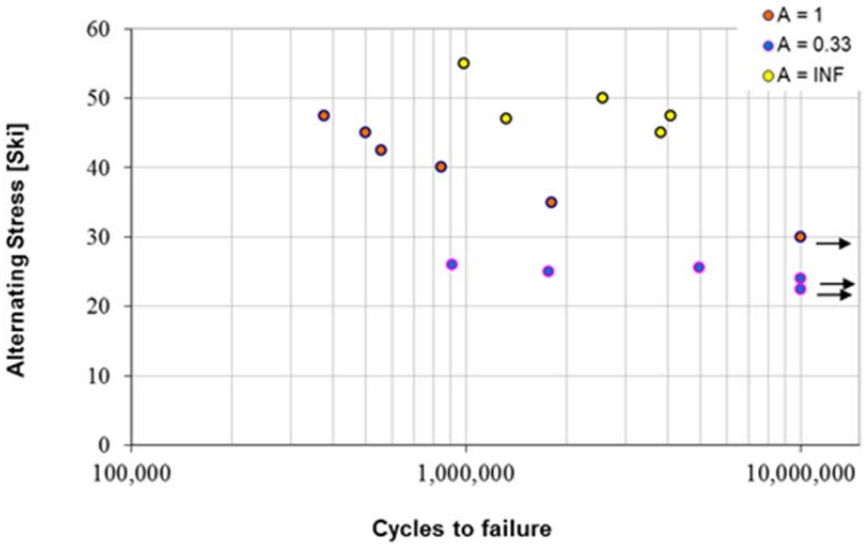

Figure 13: Alternating stress with cycles for Nimonic 105 at various A ratios

Specimens were extracted for the development of fatigue crack growth rates in Nimomic 105 for design intend. All tests were performed in accordance to ASTM E647-08, Sinusoidal Waveform and 29 Hertz. Figure 14 shows all the tests at 1200, 1300, and 1400°F (649, 704, and 760°C) and various R ratios.

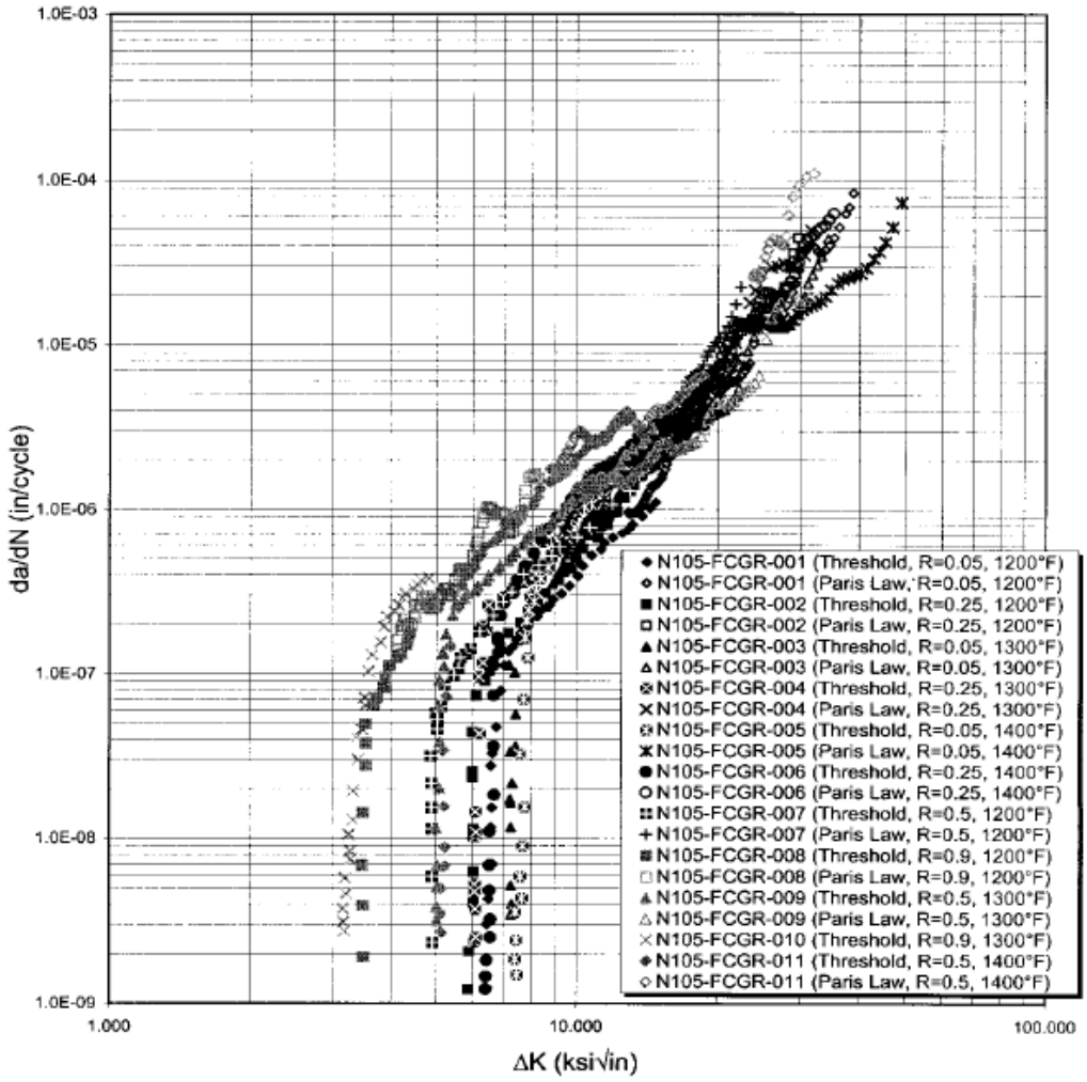

Figure 14: da/dn versus ΔK for Nimonic 105 at various temperatures & load ratio's.

Fatigue threshold data obtained from the tests are documented shown in Figure 15. The difference between the dataset in the 1200 – 1400°F (649 - 760°C) is negligible.

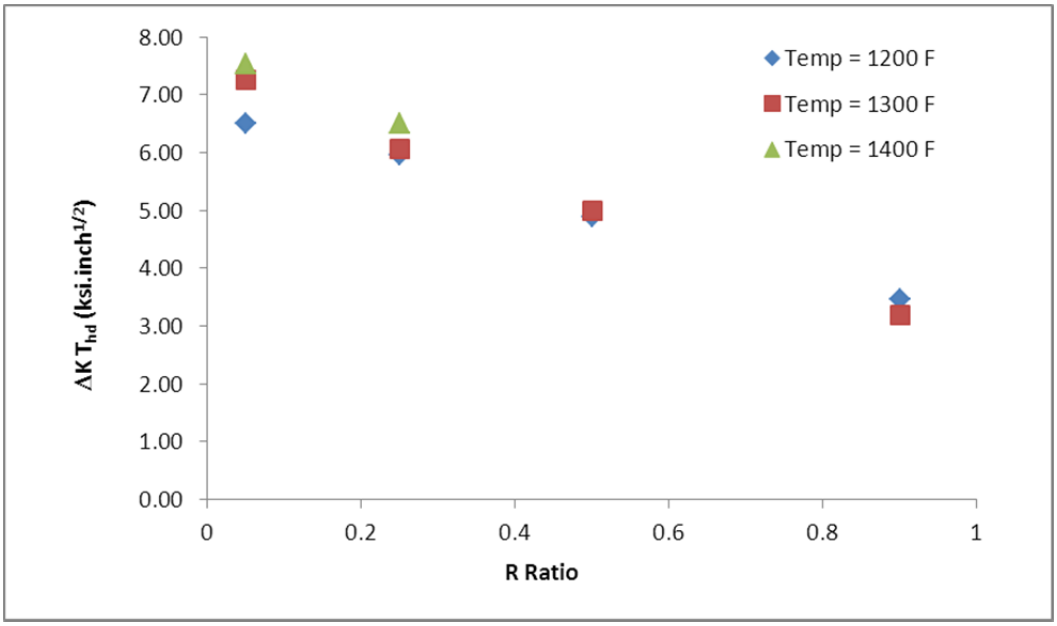

Figure 15: Figure showing fatigue threshold as a function of load ratio and temperature for Nimonic 105

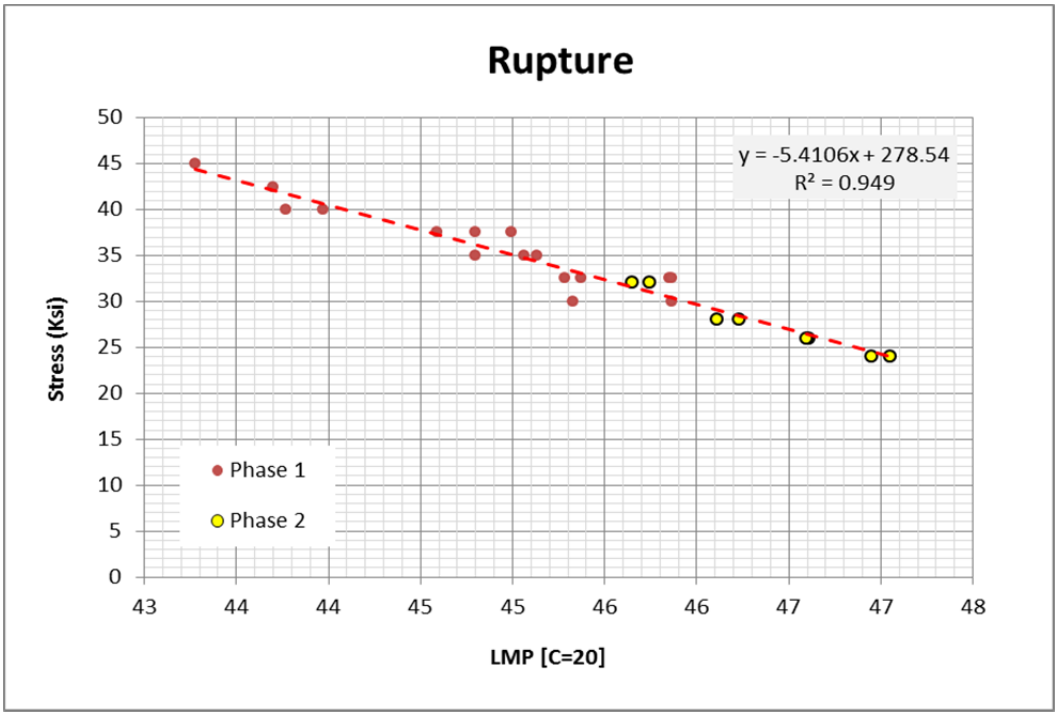

Figure 16: Larson-Miller Parameter (LMP) – Rupture Stress plot of Nimonic 105

Figure 16 shows the rupture data obtained from the long term creep testing of Nimonic 105. The times accumulated ranged from 10,000 – 35,000 hours. The plot also plots the complete dataset obtained from this program and the Phase 1 of the project**.** Figure 17 plots the strain rate versus time for failure for the specimens tested as a part of this

phase. The minimum creep rates obtained from the plot are plotted with time to rupture in Figure 18.

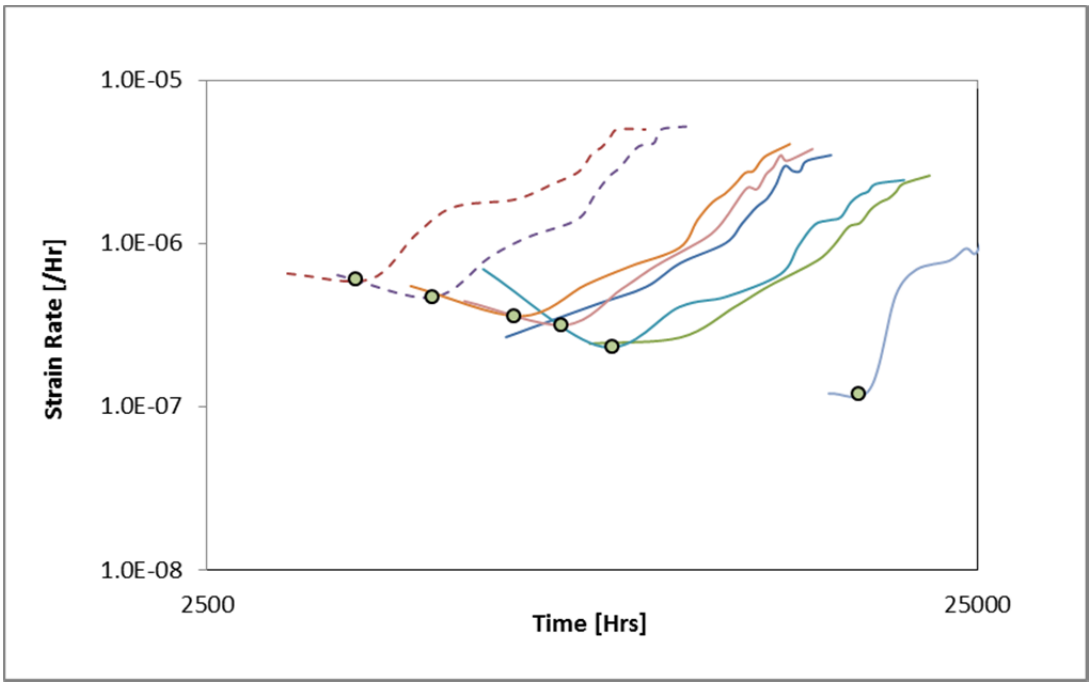

Figure 17: Plots of creep rate as a function of time

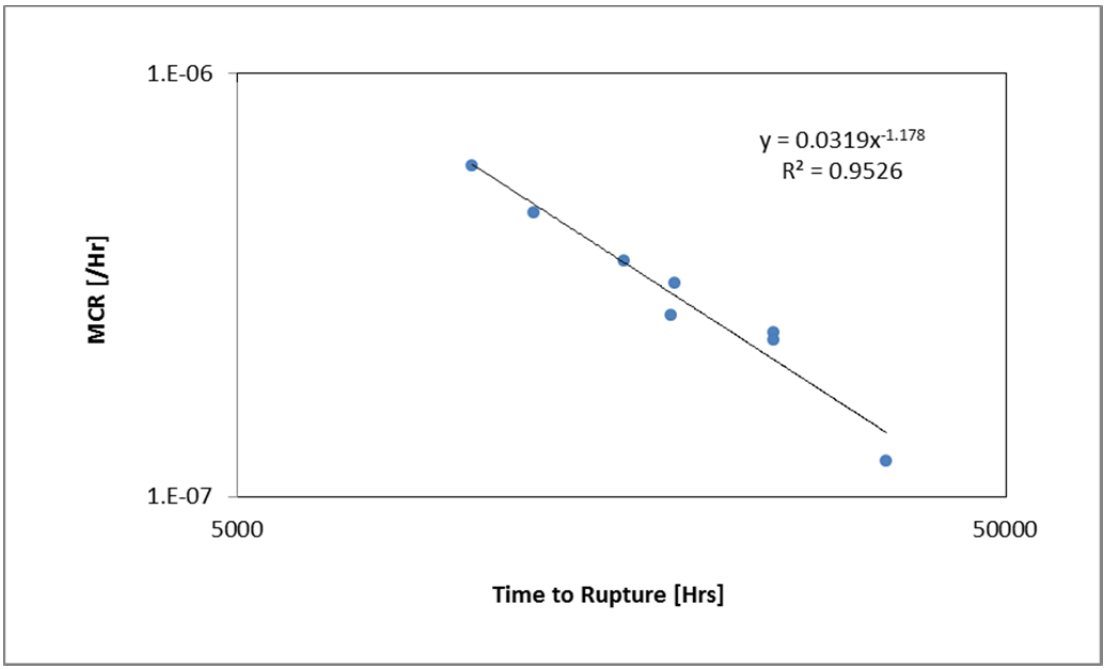

Figure 18: MCR [min. creep rate] versus time to rupture for Nimonic 105

Figure 19 and Figure 20 show the plots of 0.2% creep strain and 1% creep strain in the LMP form. The graphs also include the Phase 1 data as a composite plot covering a broad range of stress.

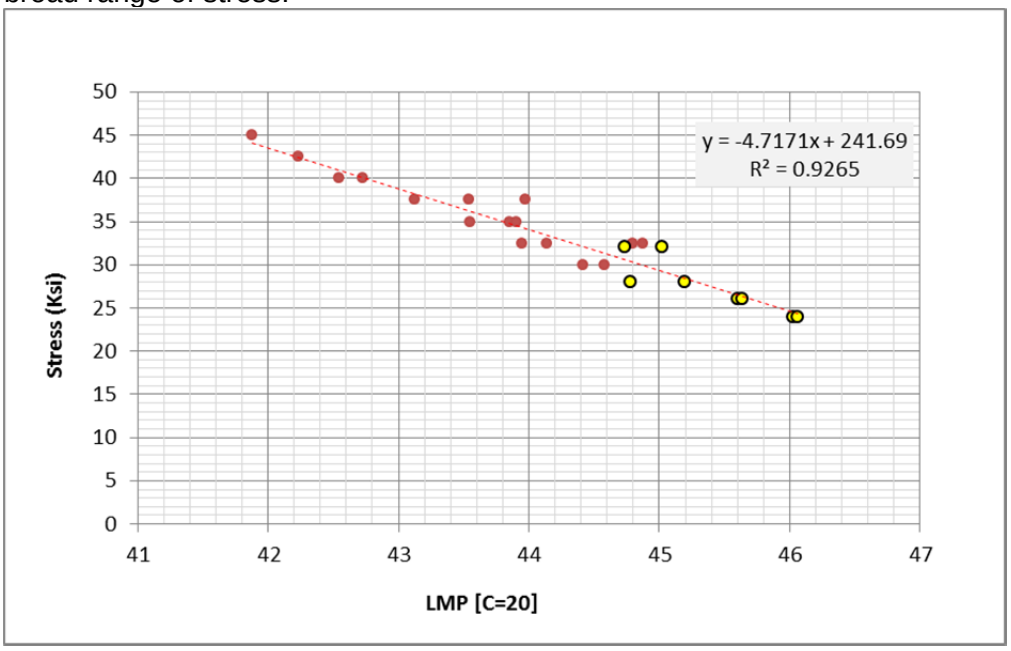

Figure 19: LMP plot of time to reach 0.2% Strain and Stress [Ksi]

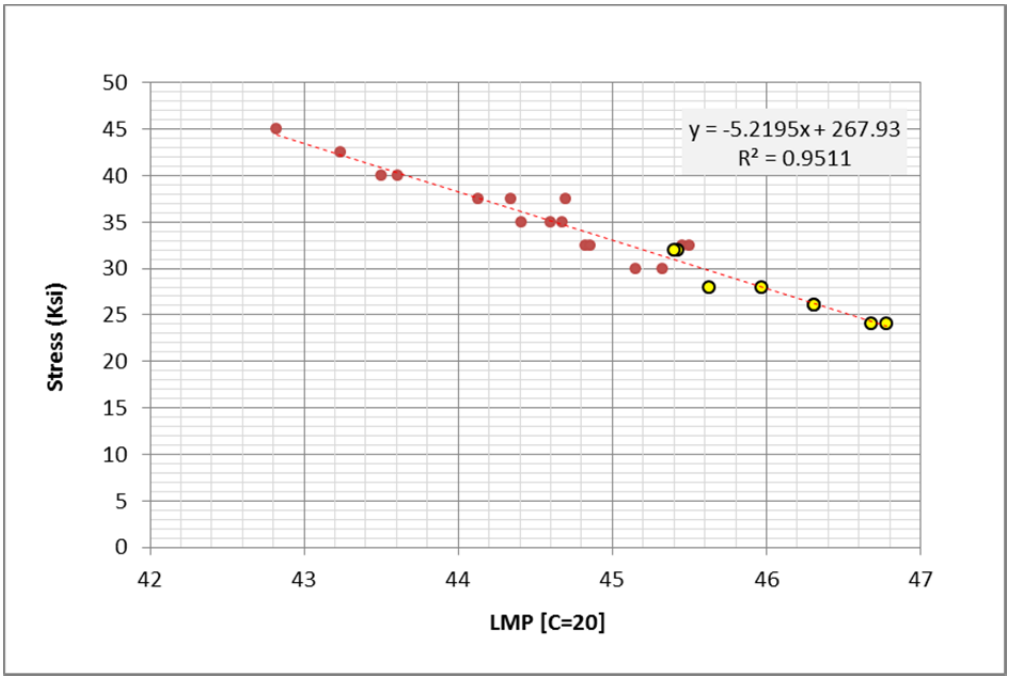

Figure 20: LMP plot of time to reach 1.0% Strain and Stress [Ksi]

The creep specimens from this program were submitted to the GE Global Research Center to ascertain the underlying creep mechanism in the specimens. Figure 21 shows the underlying dominant creep mechanisms in a succinct table.

unpaired dislocations: climb may be present but cannot observe

N105CRP-008 1400F	N105-CRP-007 1425F	N105-CRP-004 1450F	N105-CRP-002 1475F	N105-CRP-001 1500F
high density of continuous faulting/ microtwinning ½<110> pairwise shear unpaired dislocations – cross slip	unpaired dislocations - cross slip, looping ½<110> pairwise shear	unpaired dislocations - cross slip, looping ½<110> pairwise shear shear localization in g channels (formation of long γ channels)	unpaired dislocations - cross slip, looping ½<110> pairwise shear shear localization in g channels (formation of long γ channels) limited continuous faulting	unpaired dislocations – cross slip ½<110> pairwise shear (very less)
planar	wavy	wavy	wavy	wavy
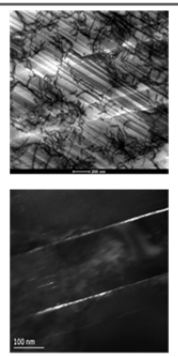	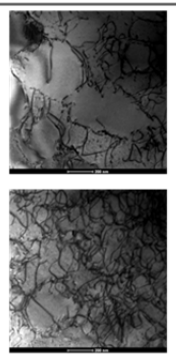	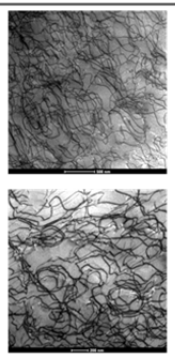	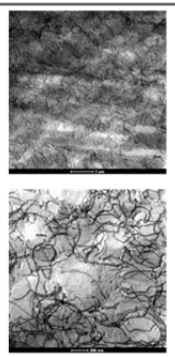	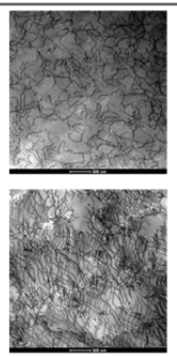

Figure 21: Dominant Creep Mechanism in N105

EVALUATION OF COMMERCIALLY AVAILABLE HAYNES®282®

Pieces of material from Haynes®282® were shipped to NETL for TEM analysis of the microstructure. Figure 22 and Figure 23 show the starting g' sizes to be in the range of 67 ± 15.5 nm with $Cr_{23}C_6$ primarily decorating the grain boundary.

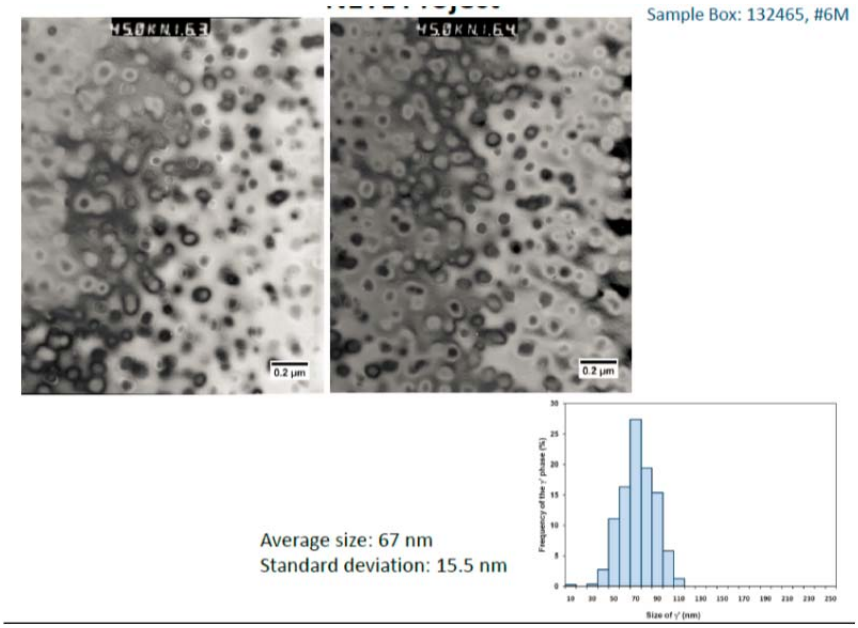

Figure 22: Typical γ' precipitate size of Haynes®282® [67 ± 15.5 nm]. (From NETL)

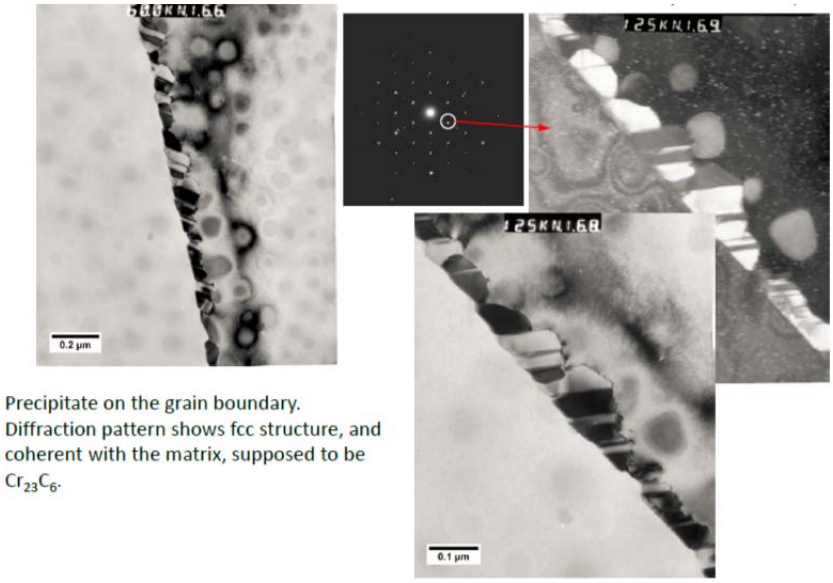

Figure 23: TEM image identifying $Cr_{23}C_6$ as a carbide phase in Haynes®282®. (From NETL)

Pieces from the Haynes®282® were exposed to 1425°F (774°C) for a period of 1 and 2 years and the properties evaluate. Figure 24 - Figure 28 show the properties obtained as a function of thermal exposure.

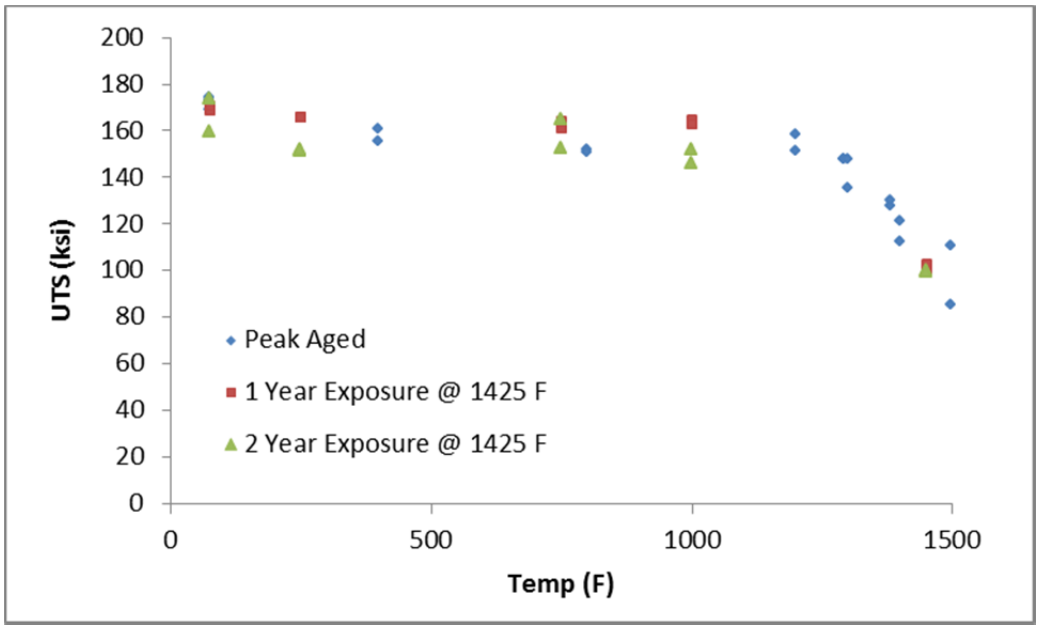

Figure 24: Tensile strength in Haynes®282® after a 1 & 2 year thermal exposure at 1425°F (774°C) [*Longitudinal Orientation*]

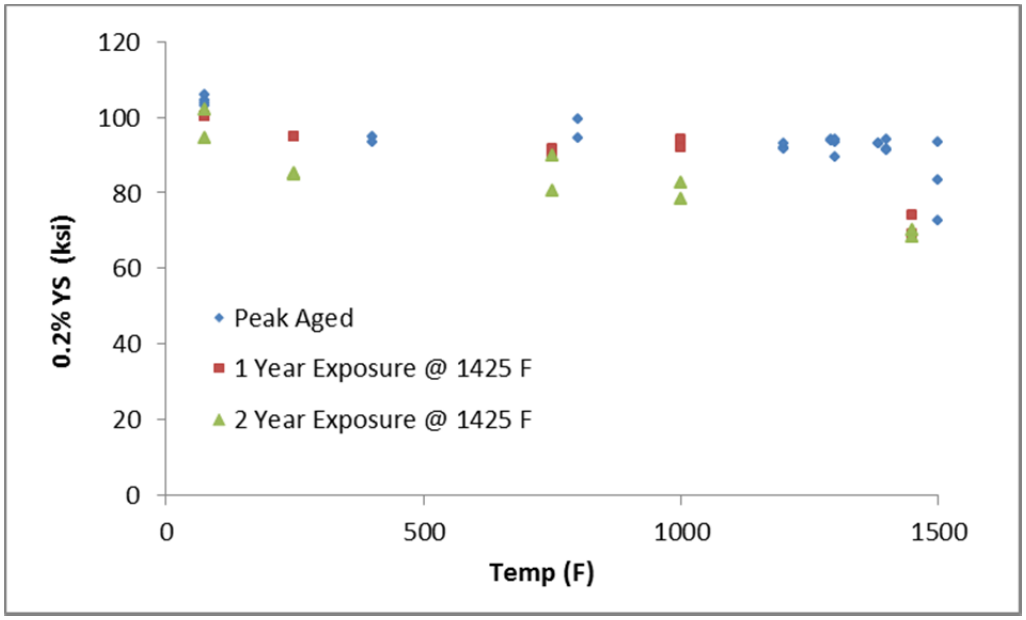

Figure 25: 0.2% Yield Strength in Haynes®282® after a 1 & 2 year thermal exposure at 1425°F (774°C) [*Longitudinal Orientation*]

Negligible drops in tensile properties [UTS and 0.2%YS] were obtained. Similar to the property drops in N105, Haynes®282® exhibited a drop in % Elongation and % RA that plateaued after a year of thermal exposure. The fracture toughness did not exhibit any deterioration in properties.

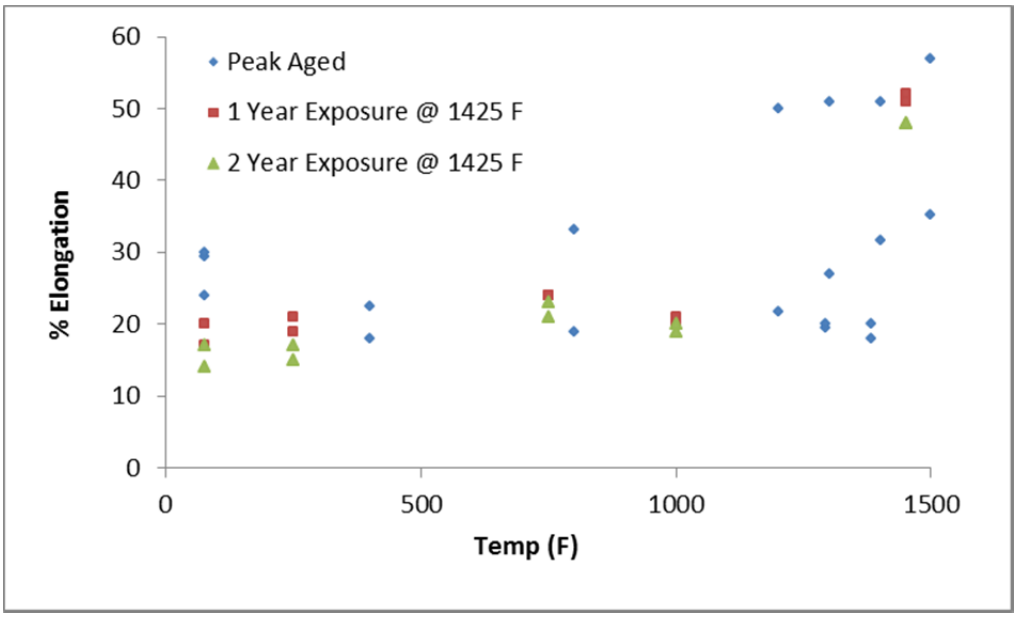

Figure 26: % Elongation in Haynes®28²® after a 1 & 2 year thermal exposure at 1425°F (774°C) [*Longitudinal Orientation*]

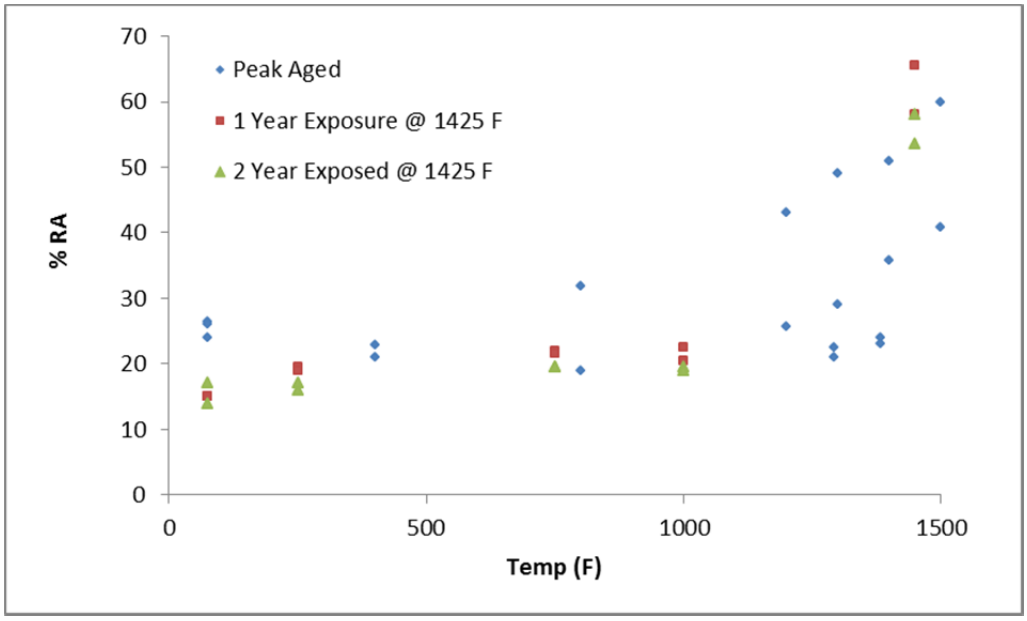

Figure 27: % RA in Haynes®28²® after a 1 & 2 year thermal exposure at 1425°F (774°C) [*Longitudinal Orientation*]

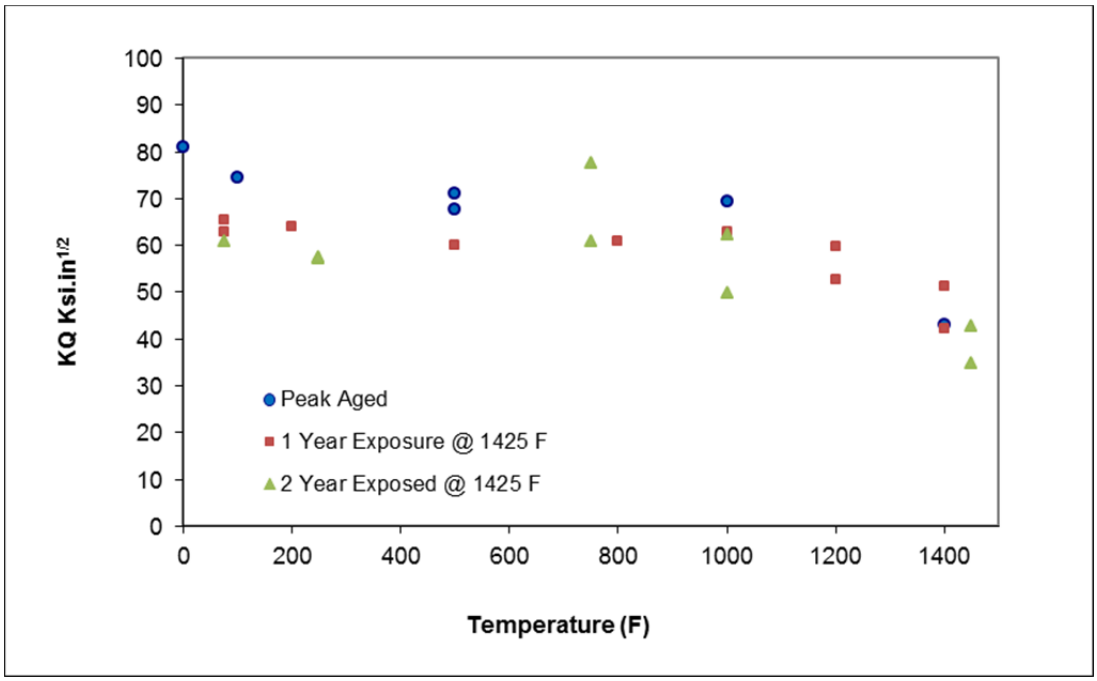

Figure 28: KQ or Conditional Fracture toughness of Haynes®282® after 1 & 2 year thermal exposure at 1425°F (774°C)

Multiple specimens were extracted from the bar for fracture toughness testing. The specimens were 0.75" thick [B] & 1.5" Wide [W]. All specimens were side grooved to a depth equal to 20% of the nominal thickness [10% each side]. The specimens were tested in accordance to ASTM E1820-09. As specimens had a mix of valid and invalid J1c, Figure 28 plots only the conditional fracture toughness of Haynes®282® as a function of temperature and thermal exposure. No debit was observed during the thermal exposure of Haynes®282® over a two year period at 1425 F.

Fatigue specimens were machined from the bar [longitudinal orientation only] and subjected to high cycle fatigue tests [in air]. All tests were performed at 1400°F (760°C), 50 Hertz and 10,000,000 cycles runout. Figure 29 shows the plot of alternating stress and cycles to failure for various A ratios.

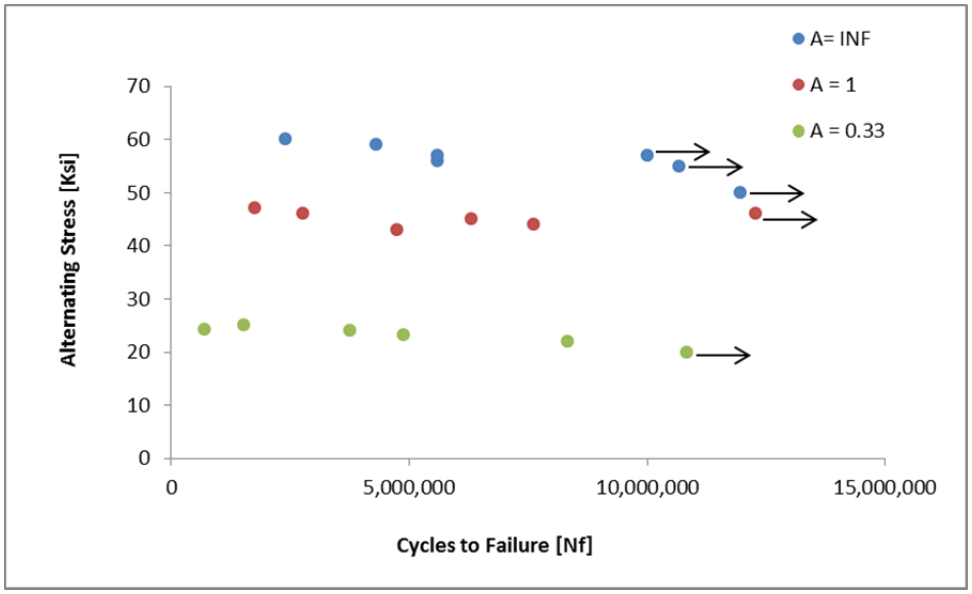

Figure 29: Figure showing alternating stress and cycles to failure at various A ratios

Hold time fatigue tests were performed on the material by hold the fatigue specimens at peak strain [a trapezoid waveform]. Such type of failure mechanism could emanate due a combination of mechanical and thermal stresses at certain locations in a component. Figure 30 shows the debit associated with the hold time fatigue of commercially available material when subjected to a 6 hour hold [plateau in the trapezoid waveform] at peak strain. Baseline data was obtained from Phase 1.

The drop in life associated with an interaction of creep and fatigue is indicative of issues that need to be accounted for during the detailed design of a component.

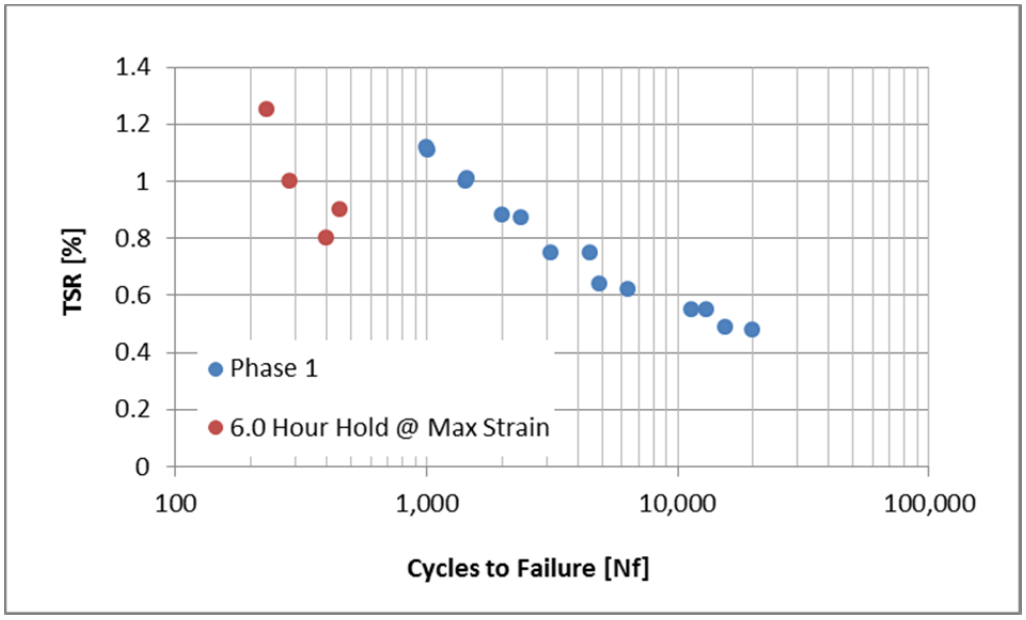

Figure 30: Debit in Hold Time Fatigue of Haynes®282®

FORGEABILITY OF COMMERCIALLY AVAILABLE HAYNES®282® FOR SMALLER FORGINGS

Haynes®282® is also a potential choice for smaller forgings in a turbine [along with Waspaloy, Nimonic 263 and Inconel 740]. The ability to forge an alloy is the determination of the appropriate temperature and strain required to achieve an appropriate grain structure that meets or exceeds the requirements of the component. A cylindrical specimen with 0.5" diameter x 1.00" Height was heat treated to 1850°F (1010°C) for 2 hours and air cooled prior to compression testing. Following was the sequence for the generation of flow stress data and the microstructural evolution.

The piece was compression tested at multiple strains [0.001 – 3.2 /sec] and multiple temperatures [1600 – 2000°F or 871 - 1093°C].

- All the specimens were heat-treated at 1850F/2hrs + air-cooled prior to compression testing.
- Compression tests have been performed at 5 temperatures - 1600°F, 1700°F, 1800°F, 1900°F and 2000°F (871°C, 927°C, 982°C, 1038°C, and 1093°C).
- Tests have been done at strain rates of 0.001, 0.01, 0.1, 1.0 and 3.2/s for each temperature
- Compression-tested specimens were sectioned axially into four quarters.
- Two quarters from each of the compression tested specimens have been heat-treated at following temperature/time conditions:
    - 1650°F (899°C)/2hrs + air-cool
    - 2150°F (1177°C)/2hrs + air-cool
- Each of these quarters were mounted, polished and etched for microstructure evaluation
- Photomicrographs have been taken at mid-radius/mid-height location of the compression-tested specimen.
- Grain size evaluation was performed by visually comparing the photomicrographs with ASTM Grain Size Chart.

Figure 31 - Figure 35 show the true stress and true strain data at 1600, 1700, 1800, 1900 and 2000°F (871°C, 927°C, 982°C, 1038°C, and 1093°C). Table 1 is a summary of the grain structure obtained as a function of various temperatures and thermal exposure. Based on the dataset, Haynes®282® exhibited evidence of duplex microstructures when re-heated to the lower temperature [< 1800°F or 982°C]. The grain size in the final product can be tailor made based on the combination of the imparted strain and the final desired microstructures. Some temperature and strain combinations show the tendency of the alloy to exhibited carbide banding.

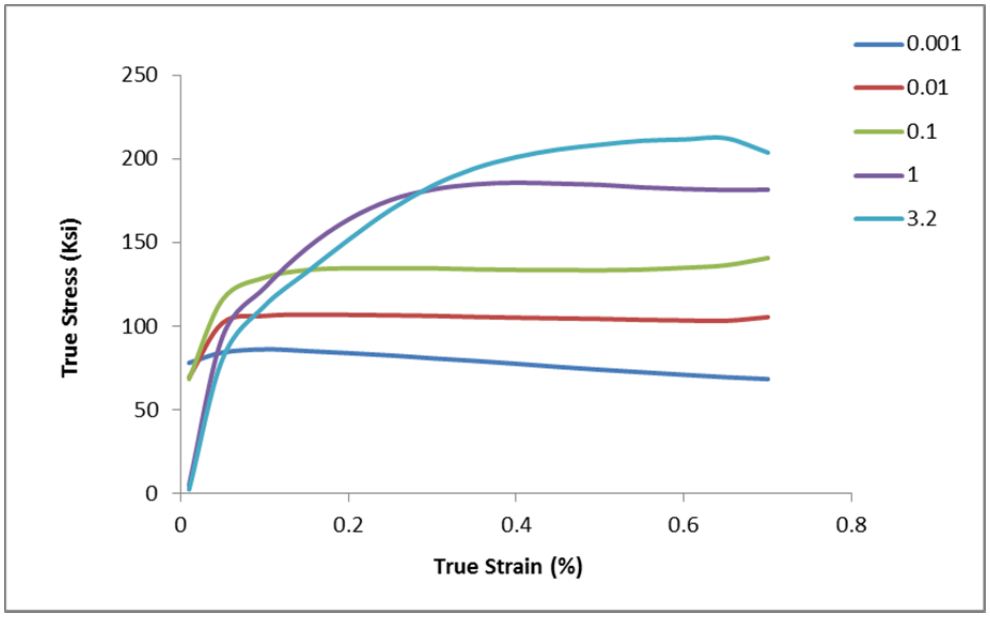

Figure 31: Flow Stress curves of Haynes®282® at 1600°F (871°C)

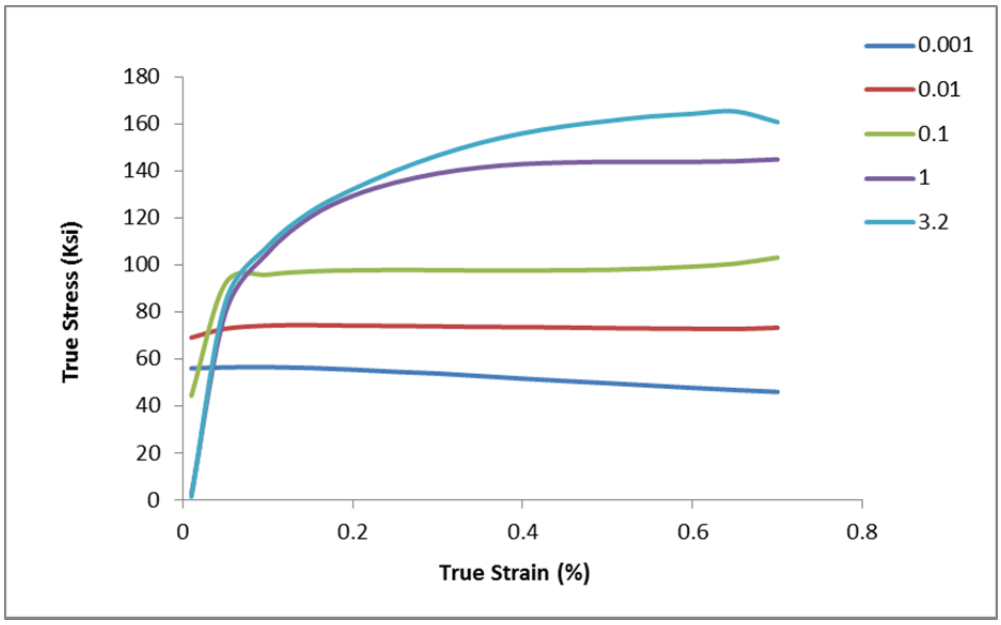

Figure 32: Flow Stress curves of Haynes®282® at 1700°F (927°C)

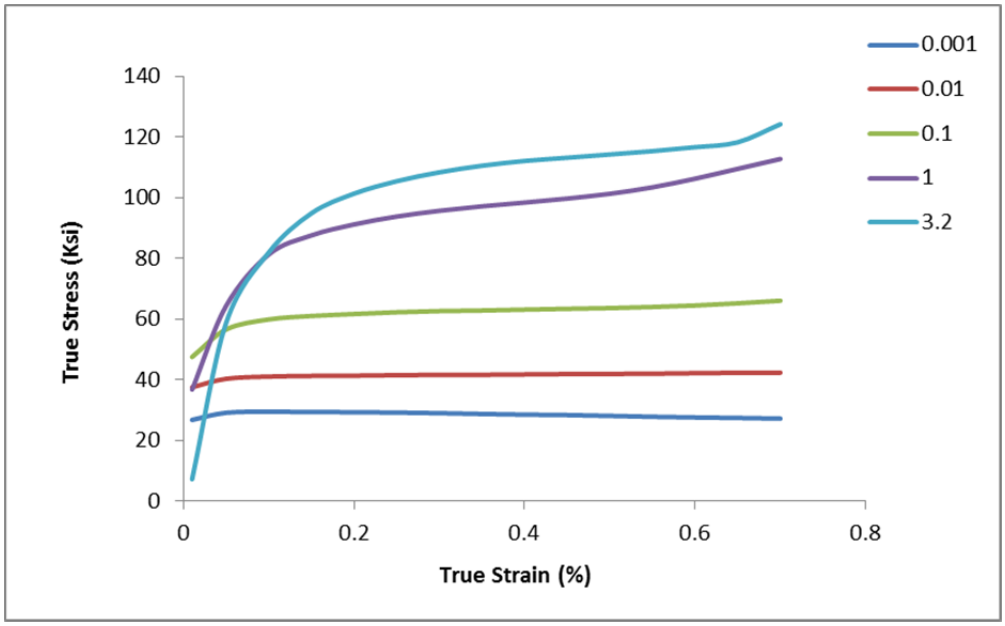

Figure 33: Flow Stress curves of Haynes®282® at 1800°F (982°C)

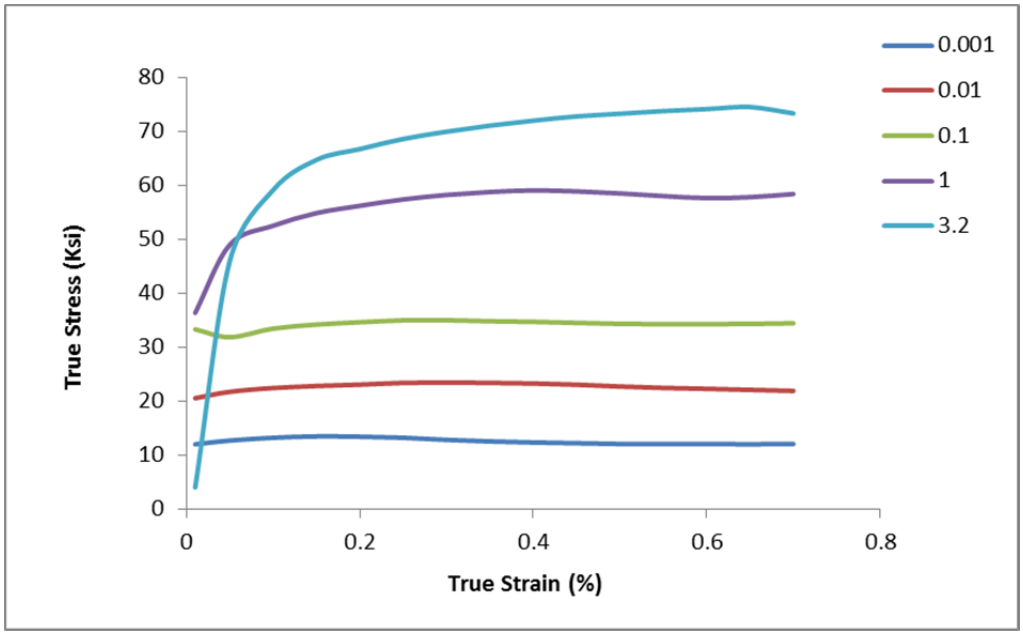

Figure 34: Flow Stress curves of Haynes®282® at 1900°F (1038°C)

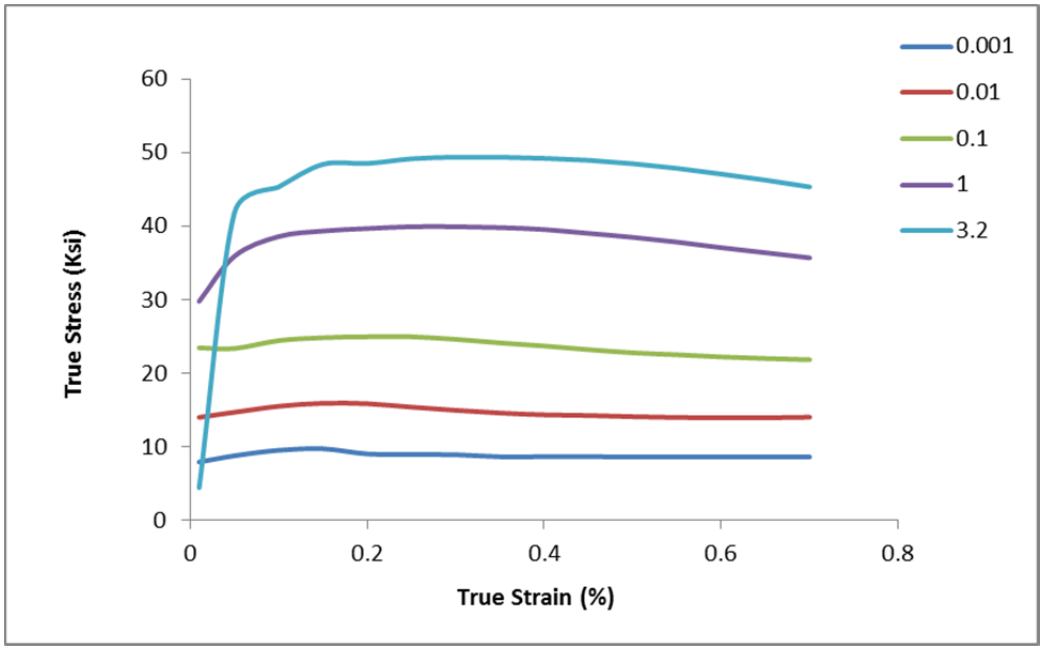

Figure 35: Flow Stress curves of Haynes®282® at 2000°F (1093°C)

Table 1: Grain size after compression tests and exposing the pieces at various temperatures for 2 hours of Hayne®282®

Compression Temperature	Re-heat Temperature (@ 2hours)	Strain Rate (in/in/sec)				
		0.001	0.01	0.1	1	3.2
1600	1650	ASTM 6 ALA 5	ASTM 8.5 ALA 4	ASTM 7 ALA 4	ASTM 5 ALA 4	ASTM 8.5 ALA 3
	1800	ATM 7.5 ALA 6.5	ATM 7.5 ALA 6.5	ASTM 10 ALA 8	ASTM 6 ALA 5	ASTM 8.5 ALA 6
	2150	ASTM 1 ALA 0	ASTM 2 ALA 1	ASTM 1 ALA 00	ASTM 1 ALA 0	ASTM 1 ALA 0
1700	1650	ASTM 5 ALA 4	ASTM 5 ALA 4	ASTM 7.5 ALA 6	ASTM 5 ALA 4	ASTM 7 ALA 6
	1800	ASTM 5 ALA 4	ASTM 5 ALA 4	ASTM 7 ALA 6	ASTM 5 ALA 4	ASTM 7.5 ALA 6
	2150	ASTM 1.5 ALA 0.5	ASTM 2 ALA 1	ASTM 1.5 ALA 0	ASTM 1.5 ALA 1	ASTM 2 ALA 0
1800	1650	ASTM 5.5 ALA 4	ASTM 6 ALA 5.5	ASTM 3.5 ALA 1	ASTM 5 ALA 4	ASTM 7 ALA 6
	1800	ASTM 5.5 ALA 4.5	ASTM 7 ALA 6	ASTM 5 ALA 4	ASTM 6 ALA 5	ASTM 7.5 ALA 6.5
	2150	ASTM 1.5 ALA 1	ASTM 2 ALA 1	ASTM 2.5 ALA 1	ASTM 1.5 ALA 1	ASTM 2 ALA 0.5
1900	1650	ASTM 9 ALA 7	ASTM 11 ALA 4	ASTM 10 ALA 9	ASTM 9 ALA 8	ASTM 9 ALA 3
	1800	ASTM 8.5 ALA 7	ASTM 8 ALA 6	ASTM 9 ALA 8	ASTM 9.5 ALA 8	ASTM 9 ALA 8
	2150	ASTM 1.5 ALA 0	ASTM 2 ALA 1.5	ASTM 2.5 ALA 1	ASTM 2.5 ALA 1.5	ASTM 2 ALA 1
2000	1650	ASTM 6 ALA 5	ASTM 7 ALA 6	ASTM 8 ALA 7	ASTM 7.5 ALA 6	ASTM 7 ALA 5
	1800	ASTM 5 ALA 4	ASTM 6.5 ALA 5.5	ASTM 7 ALA 6	ASTM 7 ALA 6	ASTM 6 ALA 5
	2150	ASTM 2.5 ALA 1	ASTM 1.5 ALA 0.5	ASTM 2 ALA 1	ASTM 1.5 ALA 1	ASTM 1 ALA 0

TRIPLE MELTING OF HAYNES®282® FOR LARGER FORGING

Though alloys such as Haynes®282®, Nimonic 263, Inconel 740, Waspaloy exhibit the requisite creep properties for A-USC conditions, the scalability of these alloys into larger components such as a forging have to be demonstrated. Haynes®282® was primarily developed for non-rotating component and has been processed via a double melt process [VIM-ESR], prior to the interest from this program. The double melt process limits the available starting size for very large diameter disk or forging. Historically, triple melt process is a prerequisite for the manufacture of rotating components and is extensively documented in literature.

Based on the recommendation of the design group, a capability of a final 44" diameter forging would demonstrated the maximum need of a Haynes®282® . Based on this information, it was desired to triple melt 24" diameter ingots [VIM-ESR-VAR] of Haynes®282®. Following was the sequence in the development of the triple melt process

- Two 18" VIM ingots (EX0045PW and EX0046PW) were poured [Figure 36]
  - Chemistries at the head and toe were confirmed to meet the chemistry of Haynes®282® [Table 2]
- The ingots were then ESR melted into 22" diameter ingots [Figure 36]
- ESR ingot EX0045PW was re-melted via VAR into a 24" diameter ingot [Figure 36]
  - The re-melting consisted of three melt rates
  - The ingot was marked for the various conditions during the melting process
  - The ingot was then homogenized based on a temperature cycle determined by NETL. The microstructure after the homogenization cycle are document in Figure 38
  - The ingot was the forged into an 8" diameter bar for maintaining the location of the melt rates [Figure 39] and the resultant microstructure evaluated [Figure 40]
  - The 8" diameter bar was then sectioned and macro-etched with Canada's Etch to reveal segregation tendencies [Figure 41] for various melt conditions.
- The second ESR Ingot EX0046PW was then re-melted via VAR into a 24" diameter ingot with the optimum melt rates determined from the first ingot
  - The ingot was billetized into a 20" diameter bingot [Figure 42]
  - Section from the bingot EX0046PW was cut for macro-segregation (Figure 43) and microstructural analysis (Figure 44)

The 20" diameter bingot was the starting feedstock for the forge ability studies, sub-scale forgings and eventually the large 44" diameter disk of Haynes®282®. All development activities were performed by GE Power and Water and Special Metals.

18” VIM

ESR – 22” Diameter 24” Diameter VAR

Figure 36: Pictures showing the 18” VIM / 22” ESR and the final 24” VAR Ingot.

Table 2: Chemistries obtained from the Hayne®282® ingots

Element	Composition (wt. %)							
	EX0045PW Head			EX0045PW Toe			EX0046PW Head	EX0046PW Toe
	Surface	Mid-Radius	Center	Surface	Mid-Radius	Center		
C	0.065	0.061	0.061	0.056	0.064	0.063	0.061	0.061
Mn	0.034	0.033	0.033	0.033	0.033	0.033	0.033	0.034
Fe	0.849	0.794	0.815	0.767	0.763	0.812	0.49	0.49
S	0.001	0.0008	0.0008	0.0011	0.0011	0.0012	0.0005	0.0004
Si	0.056	0.059	0.057	0.067	0.066	0.064	0.057	0.067
Cu	0.023	0.022	0.022	0.023	0.023	0.024	0.024	0.024
Ni	56.67	57.23	57.07	56.76	56.72	56.54	56.85	56.85
Cr	19.58	19.32	19.42	19.56	19.58	19.42	19.65	19.64
Al	1.62	1.56	1.58	1.58	1.58	1.69	1.57	1.54
Ti	2.14	2.12	2.12	2.18	2.19	2.26	2.11	2.13
Mg	0.001	0.002	0.001	0.001	0.002	0.002	0.0007	0.0008
Co	10.26	10.25	10.26	10.26	10.24	10.25	10.30	10.29
Mo	8.56	8.41	8.43	8.57	8.60	8.70	5.56	8.57
Nb	0.083	0.082	0.080	0.079	0.080	0.081	0.079	0.08
Ta	0.0024	0.0003	0.0009	0.0017	0.0018	0.0018	0.001	0.002
P	0.0027	0.0026	0.0025	0.0026	0.0027	0.0026	0.003	0.003
Ca	0.0009	0.0009	0.0009	0.001	0.001	0.001	0.001	0.001
V	0.012	0.011	0.012	0.012	0.012	0.012	0.012	0.012
W	0.03	0.025	0.027	0.029	0.029	0.029	0.03	0.03
Zr	0.0017	0.0014	0.0014	0.0015	0.0016	0.0018	0.002	0.001
B	0.0040	0.0039	0.0039	0.0038	0.0039	0.0038	0.004	0.0039

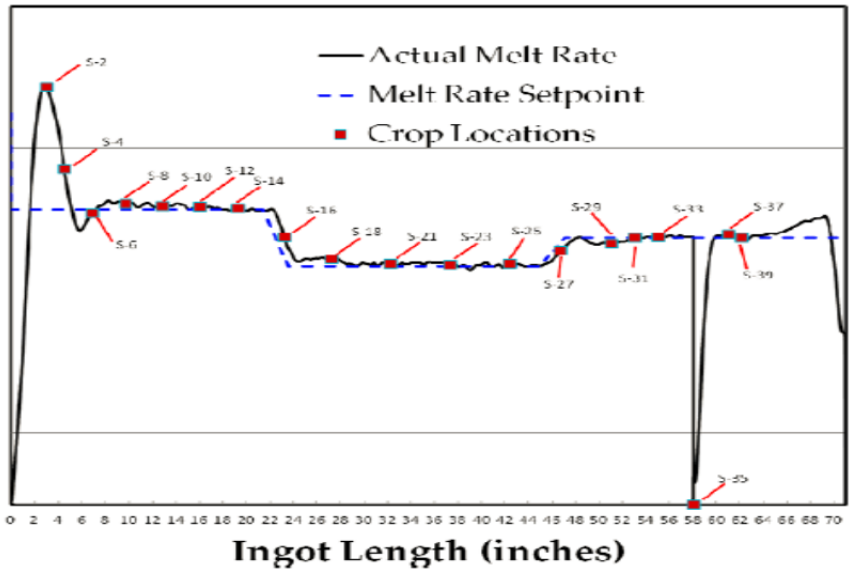

Figure 37: Variation in VAR Melt range [lbs/min] for marco evaluation

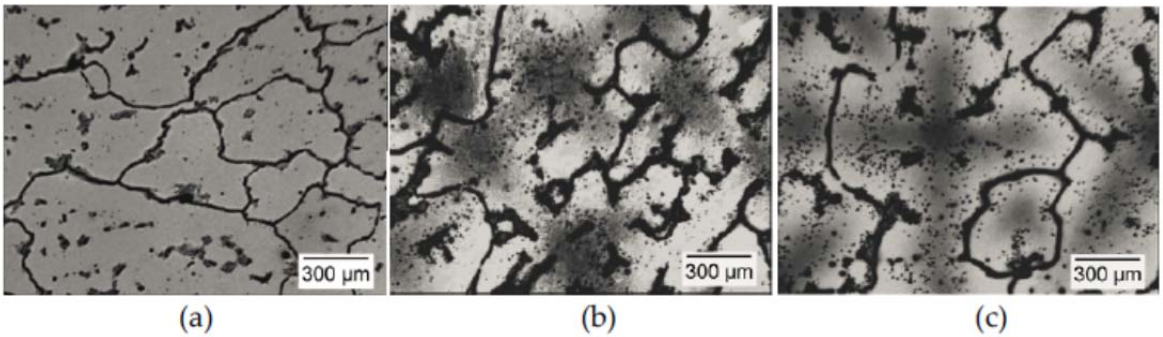

Figure 38: Representative microstructures of 24” ingot EX0045PW after homogenization

Figure 39: EX0045PW was forged into 8” diameter for macro-segregation evaluation

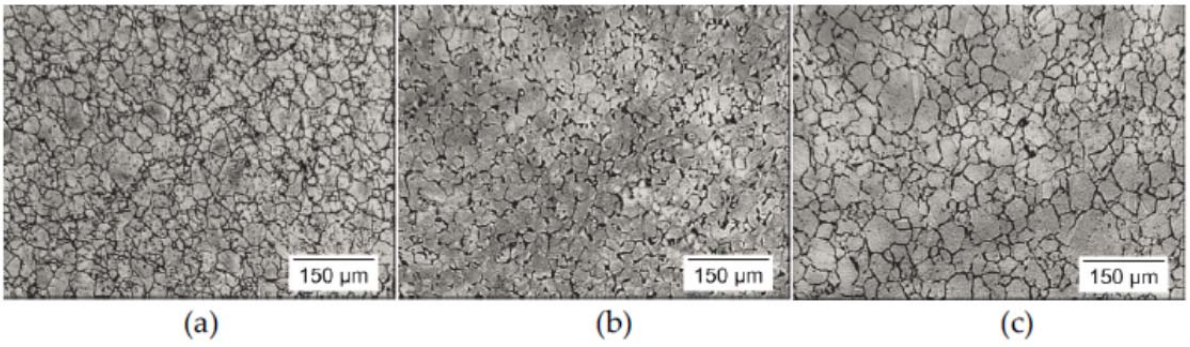

Figure 40: Representative microstructures of ingot EX0045PW after hot working to the 8” diameter bars (a) Surface (b) mid-radius and (c) center locations

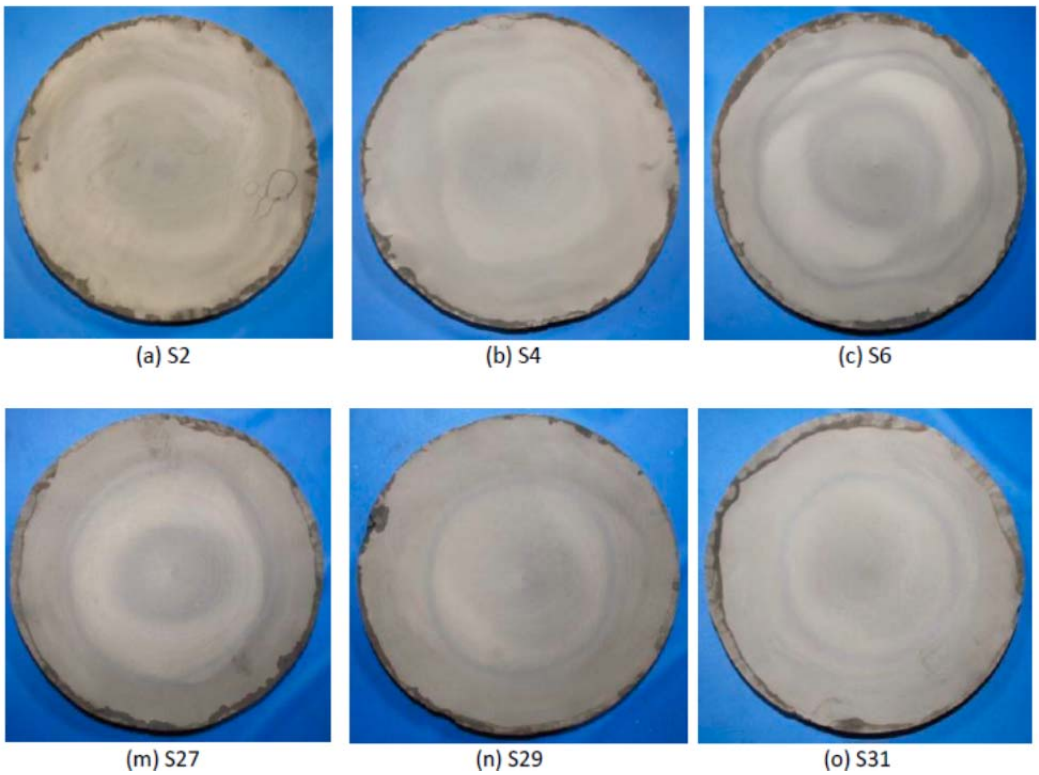

Figure 41: Representative macro slices from EX0045PW and etched with Canada's Etch to reveal segregation tendencies

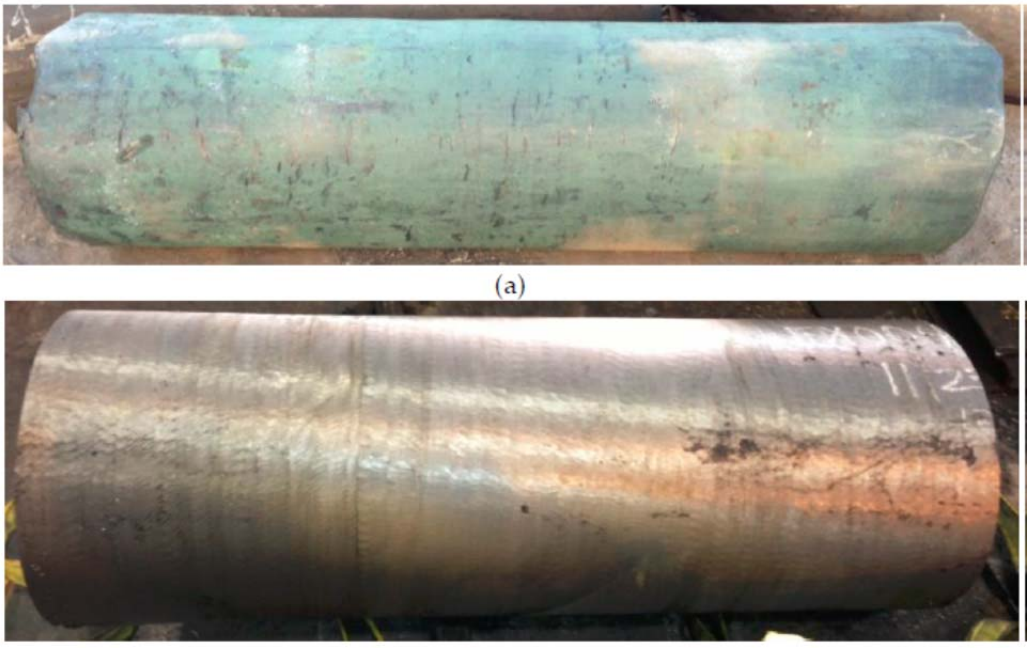

Figure 42 Second ingot EX0046PW billetized in (a) as forged condition and (b) after surface grinding to final diameter

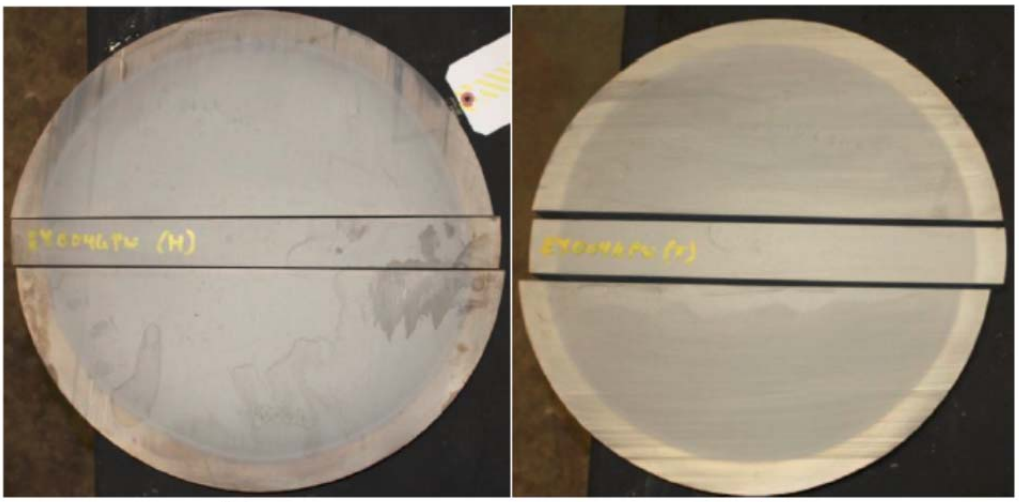

(a) (b)

Figure 43: Second ingot EX0046PW slice revealed no indication of segregation at (a) Head and (b) Toe [2]. Slices shown for microstructures

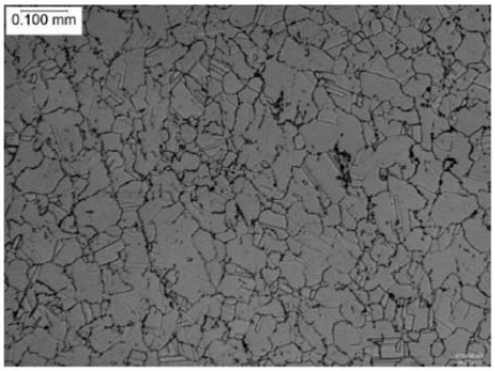

Grain Size ASTM 6 ALA 5

OD

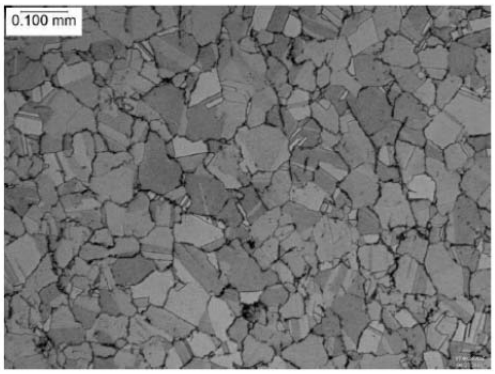

Grain Size ASTM 5

1.5” from OD

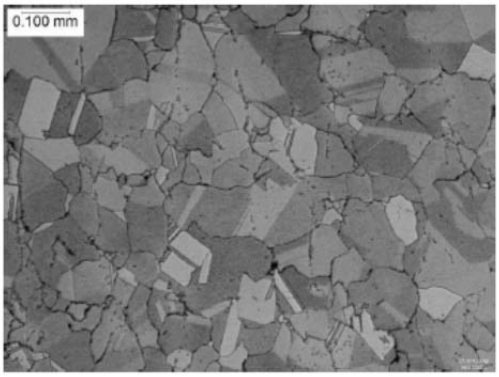

Grain Size ASTM 4 ALA 3

4” from OD

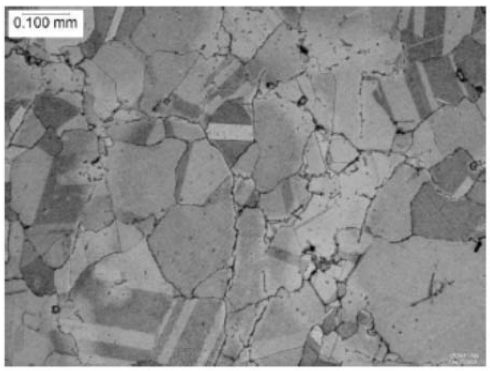

Grain Size ASTM 2.5

ID

Figure 44: Representative micro-graphs showing starting microstructure from the 20” diameter EX0046PW bingot head

LARGE FORGING OF HAYNES®282®

Multiple section of the triple melt forging was machined to characterize the microstructural stability of the alloy at various temperatures. Following were the sequence of steps followed to identify the right forging temperature and the successful demonstration of the large diameter disk of Haynes®282®

- Pieces of the bingot were exposed at various temperatures [1800, 1850, 1900, 1950 and 2000°F or 982, 1010, 1038, 1066, and 1093°C] for 4, 8 and 16 Hours
  - Figure 45and Figure 46 are representative microstructures obtained at various locations as a function of thermal hold.
  - 40 compression test specimens were machined from the billet to determine the flow stress data. The tests were performed at 1700, 1800, 1900 and 2000°F (927, 982, 1038, and 1093°C at various strain rates [0.001, 0.01, 0.1, 1 and 3.2 /sec].

- Two slugs [5" dia X 6.75"] were machined were heated and forged into pancakes in the following sequence
    - The first slug was forged at 1900°F (1038°C) two forge operation
      - Operation 1: 2:1 reduction and air cooled [Final: 6.75" dia x 3.4"]
      - Operation 2: 2:1 reduction and air cooled [Final: 3.4 dia x 1.7"]
    - The second slug was forged at 1900°F (1038°C) in a single operation
      - 4:1 reduction and air cooled [Final: 6.75" x 3.4"]

  - A 1in thick slice was removed through the diameter and a center to edge section metallographically prepared and etched. A 0.5" grid placed across the part and the grain size measured at the intercepts. Figure 47 and Figure 48 show the photomicrographs for the center, mid radius, and outer diameter.

- Based on the data and with an aim grain size of ASTM 8 and fine, the forging was obtained by a triple upset operation at 1900°F (1038°C). Figure 49 is an image showing the successful demonstration of a large diameter Haynes®282® forging.

All microstructural stability studies, sub-scale forgings and the large disk forging were performed by Wyman Gordon [Texas & Massachusetts].

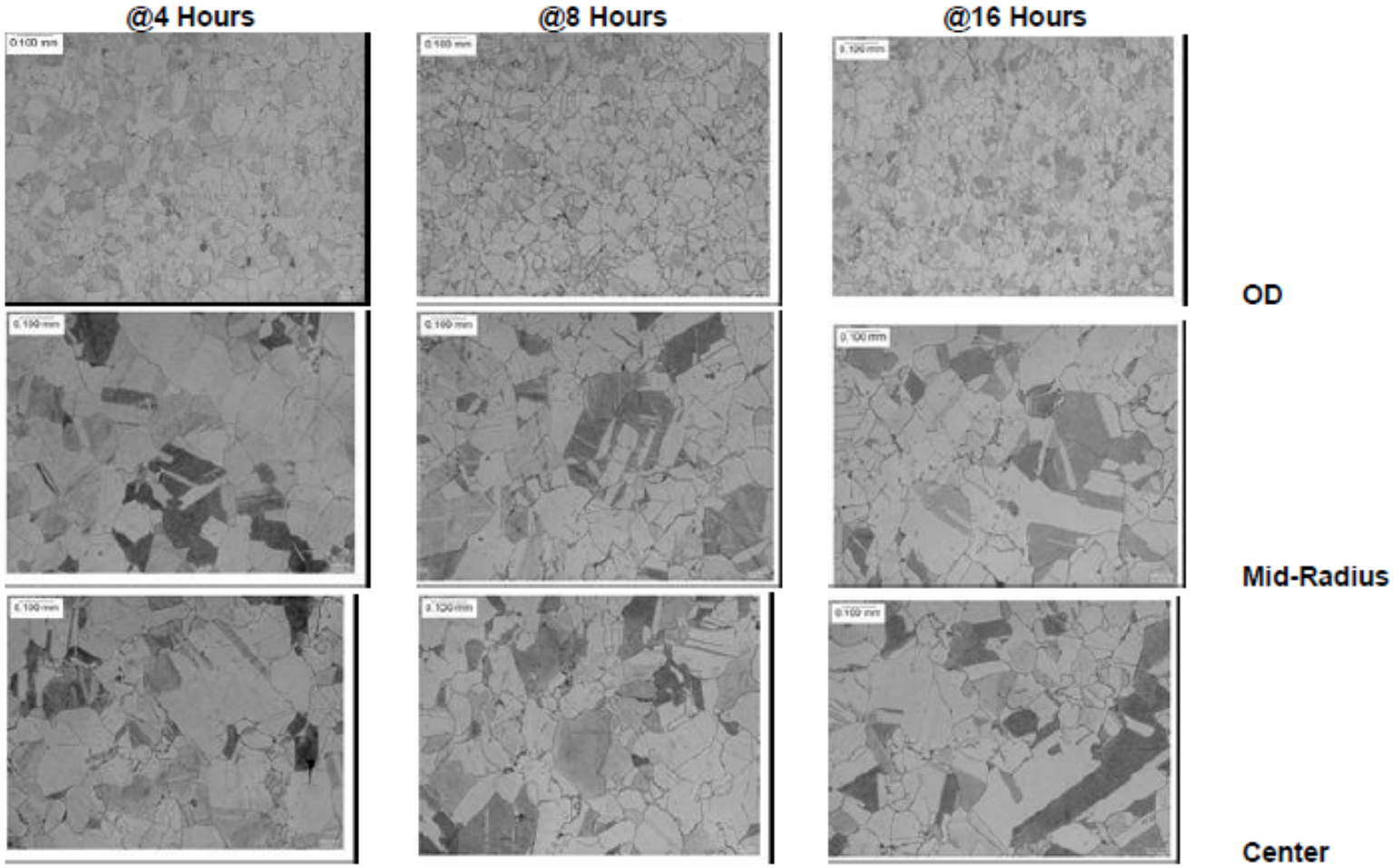

Figure 45: Coarsening studies of starting material exposed at 1800°F (982°C) at various times

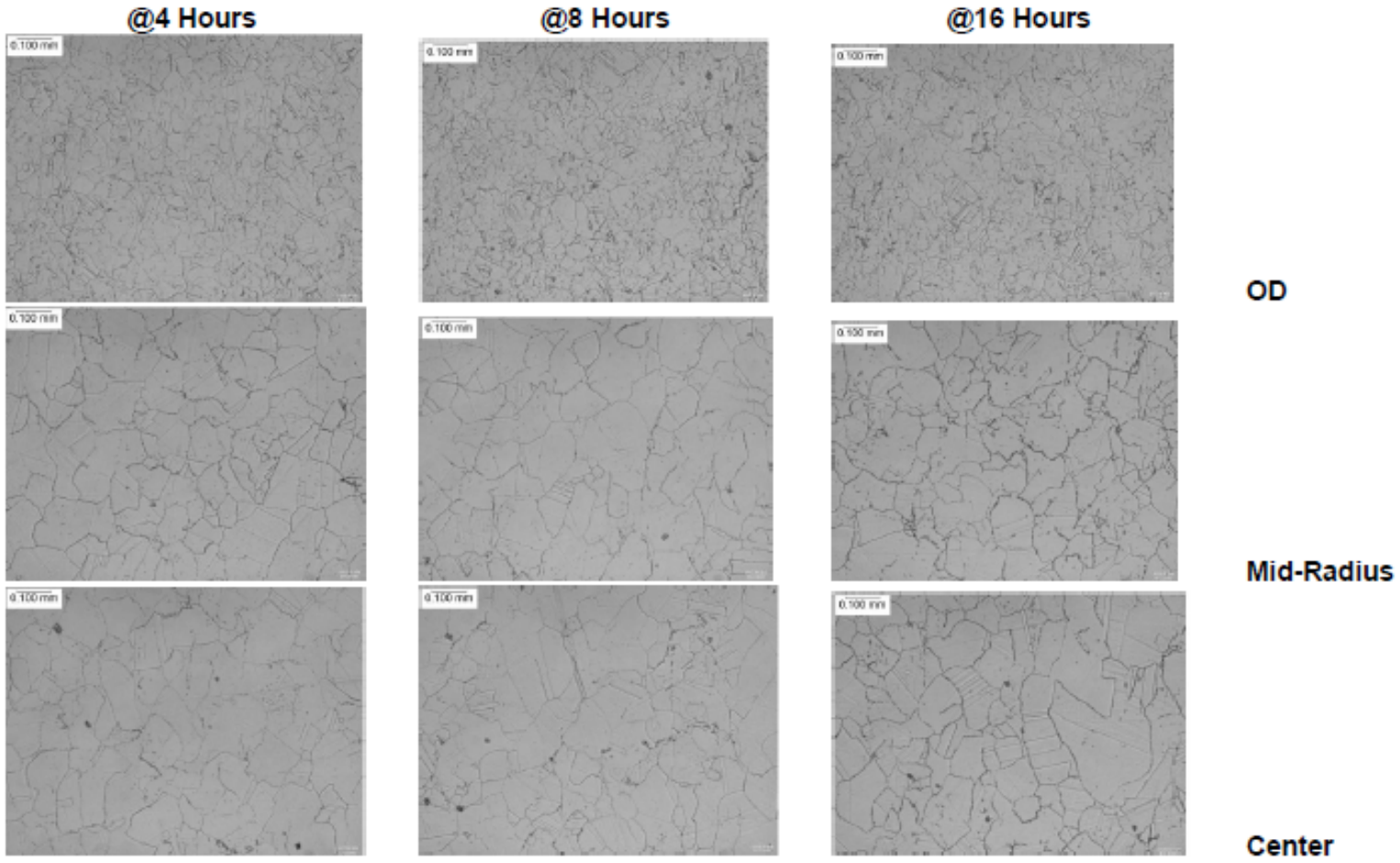

Figure 46: Coarsening studies of starting material exposed at 1900°F (1038°C) at various times

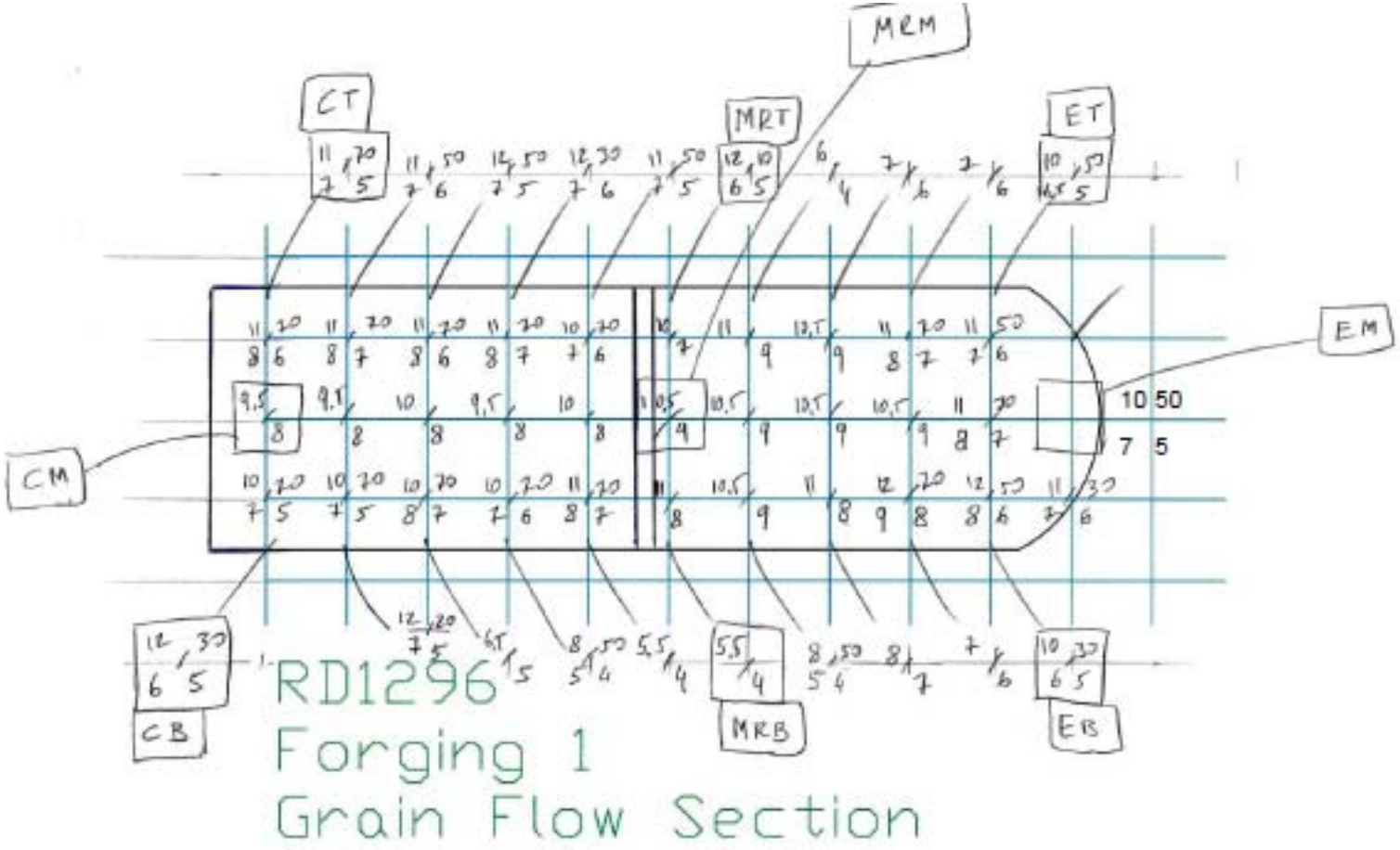

Figure 47: Grain size map of a subscale forging forged in two operations of 2:1 reduction ratio each.

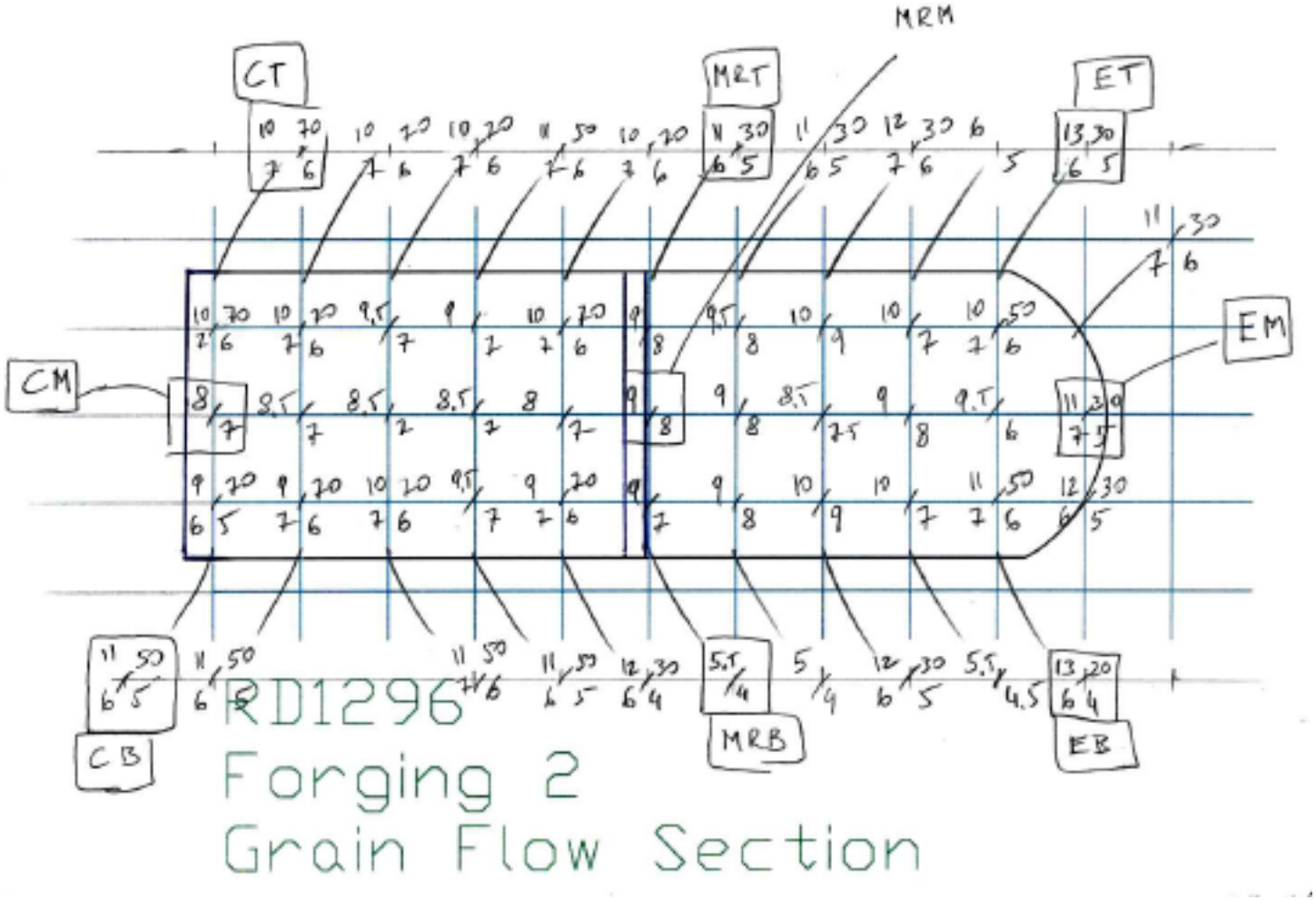

Figure 48: Grain size map of a subscale forging forged in a straight 4:1 reduction ratio.

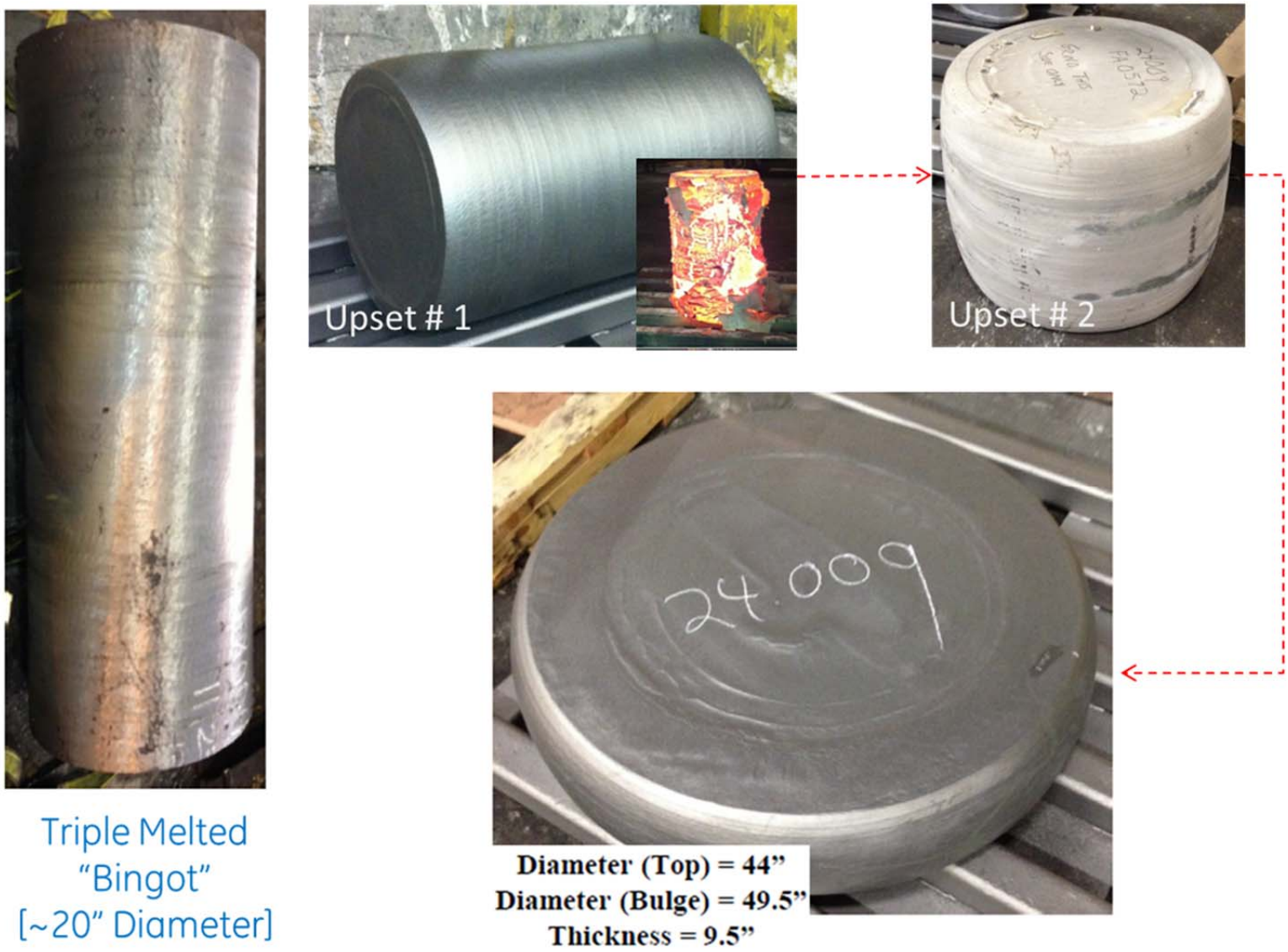

Figure 49: Demonstration of a large diameter Haynes®282® forging

CHARACTERIZATION OF THE LARGE FORGING OF HAYNES®282®

The disk obtained from Wyman Gordon was heat treated with a typical double age process.

Age 1:	1850°F (1010°C) for 2 Hours and air cooled
Age 2:	1450°F (788°C) for 8 Hours and air cooled

Multiple cuts were performed in the disk the microstructure evaluated. Figure 50 shows the typical microstructure obtained from the Haynes®282® forging. The grain size was very fine and typically ASTM 8-9, ALA 4.

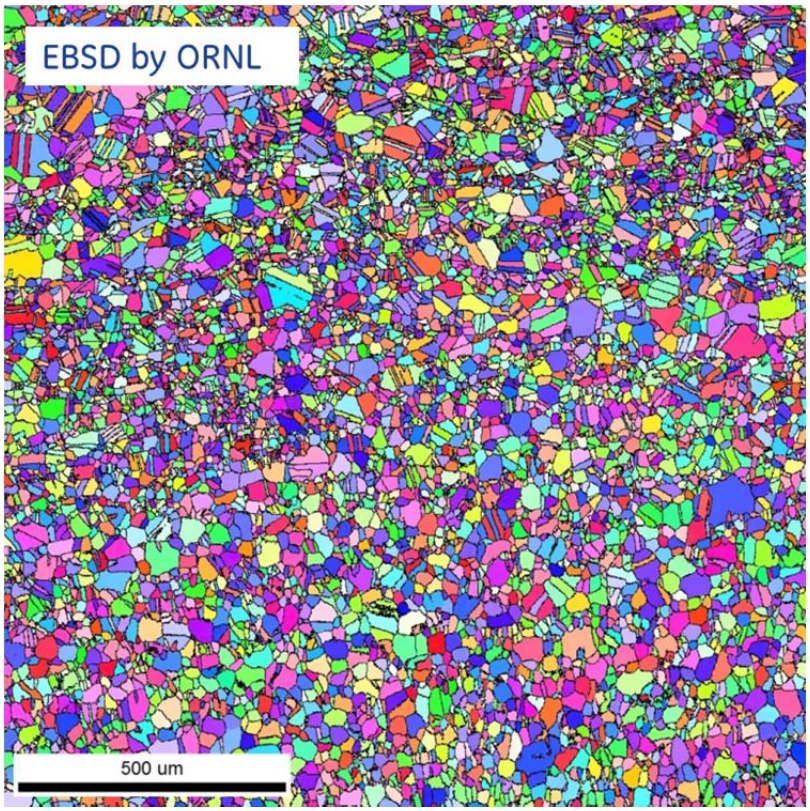

Figure 50: EBSD image of the grain size obtained in the Haynes®282® forging [Courtesy ORNL]. Typical grain size was ASTM 8-9, ALA ASTM 4

The forging was cut and multiple specimens were obtained [at various orientations] to fully characterize the forging. Figure 51 through Figure 54 show the tensile properties obtained from the disk for the radial and tangential orientation.

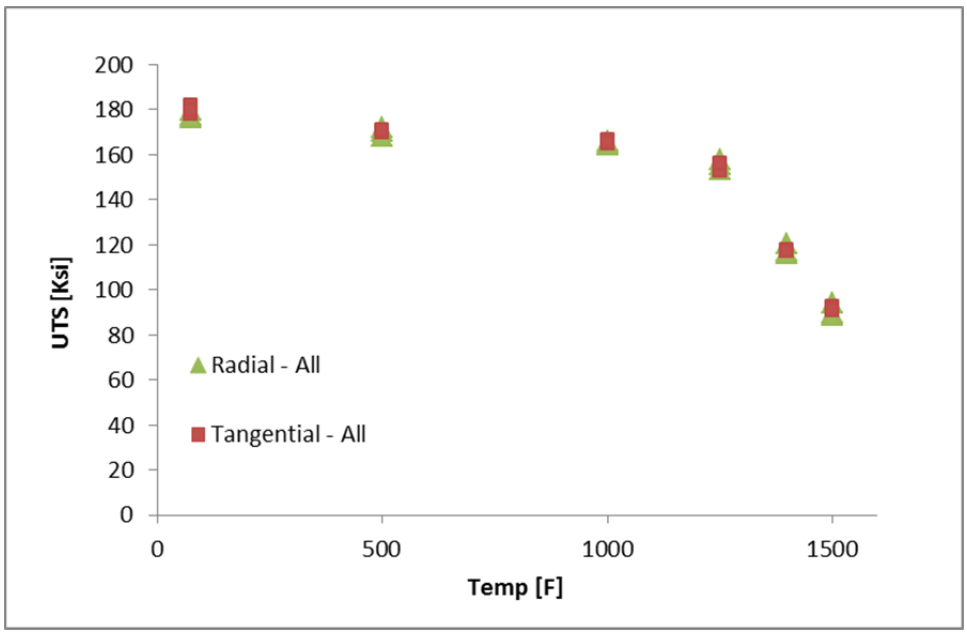

Figure 51: UTS as a function of temperature from Haynes®282® forged disk

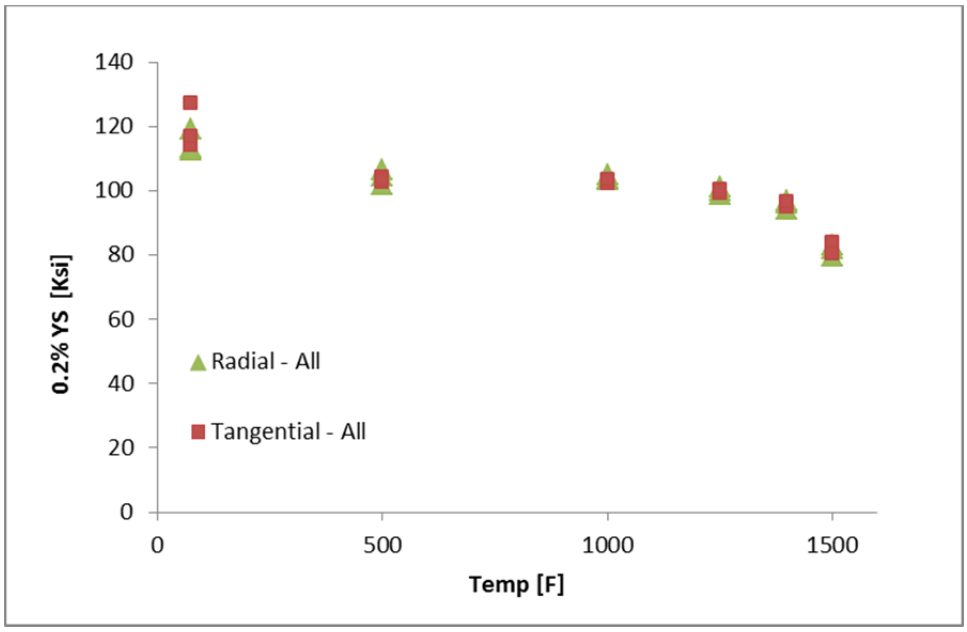

Figure 52: 0.2%YS as a function of temperature from Haynes®282® forged disk

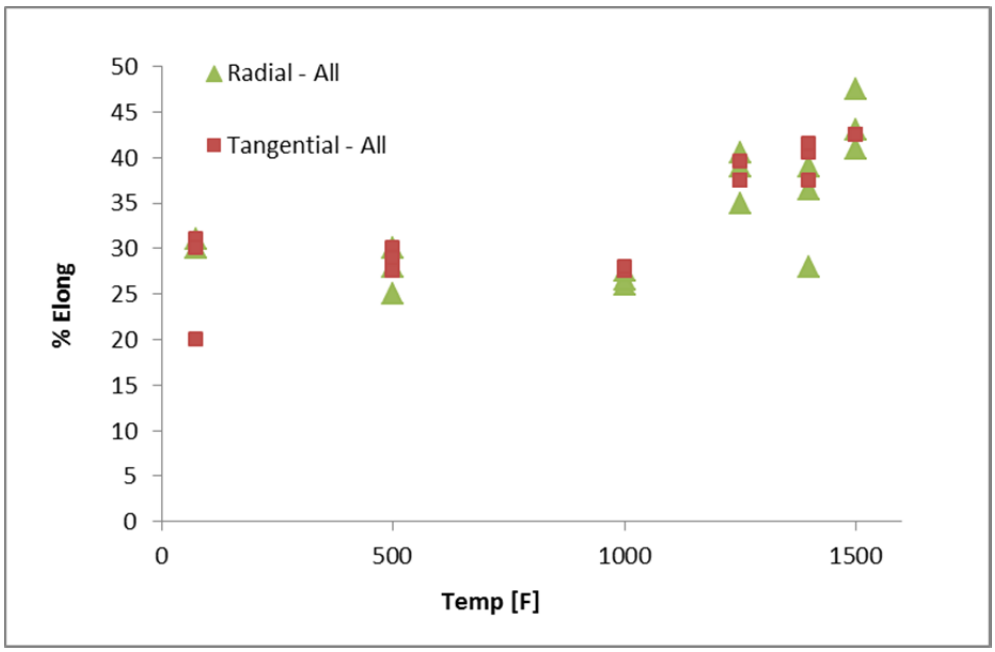

Figure 53: % Elongation a function of temperature from Haynes®282® forged disk

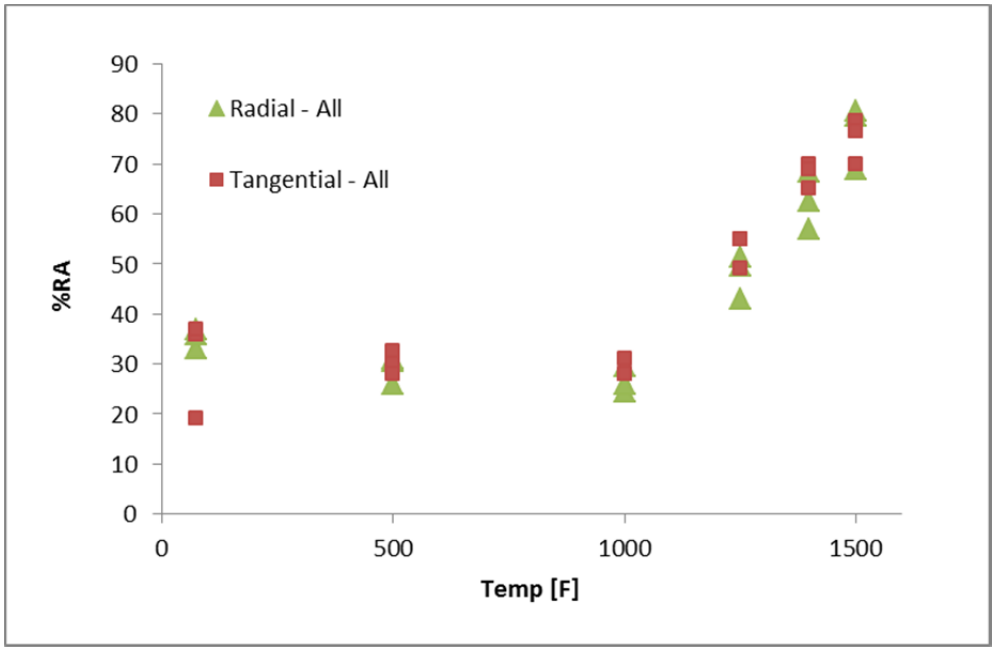

Figure 54: % RA a function of temperature from Haynes®282® forged disk

Figure 55 through Figure 57 show the high cycle fatigue results from Haynes®282® forging. The figures represent various A ratios [A=INF, 1 and 0.5] and all orientations, 1400°F (760°C), A= INF, 50 Hz and Triangular waveform. The data obtained from commercially available Haynes®282® is also plotted for reference.

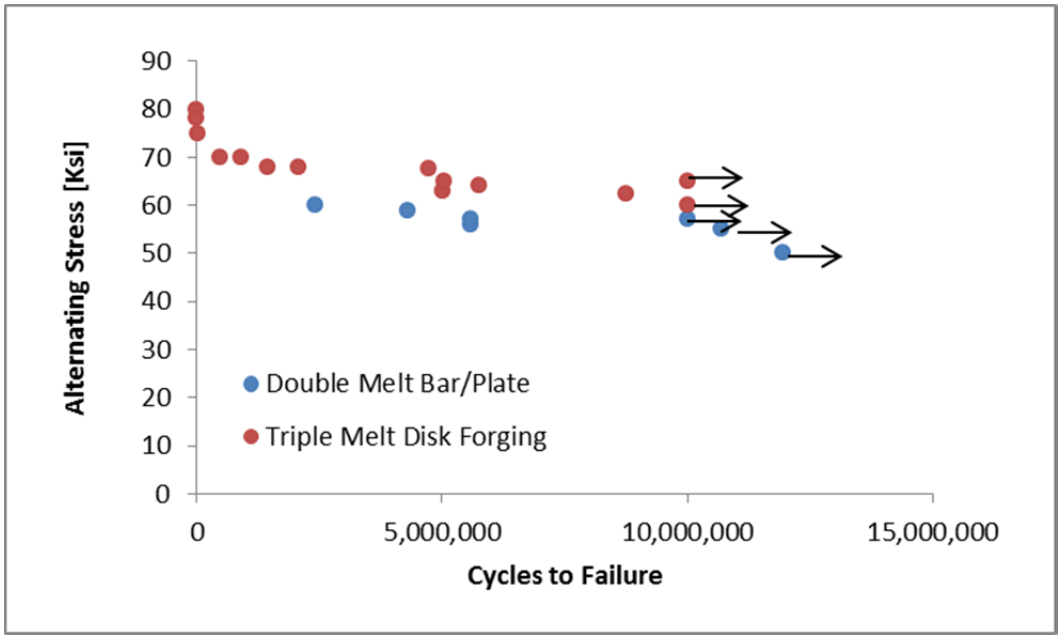

Figure 55: High cycle fatigue data from Haynes®282® disk forging [A=INF]

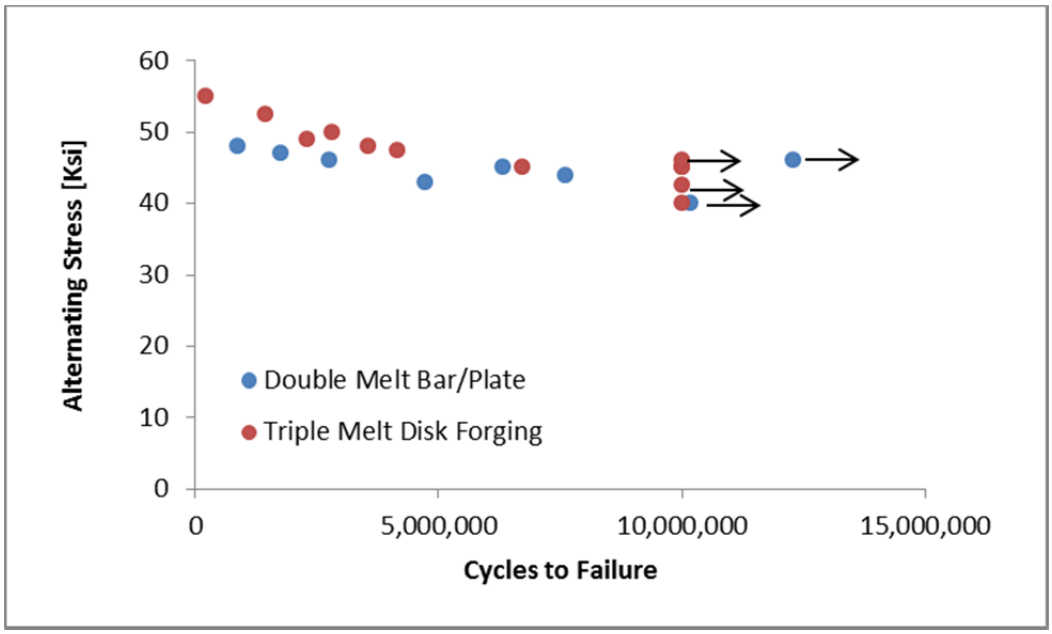

Figure 56: High cycle fatigue data from Haynes®282® disk forging [A=1]

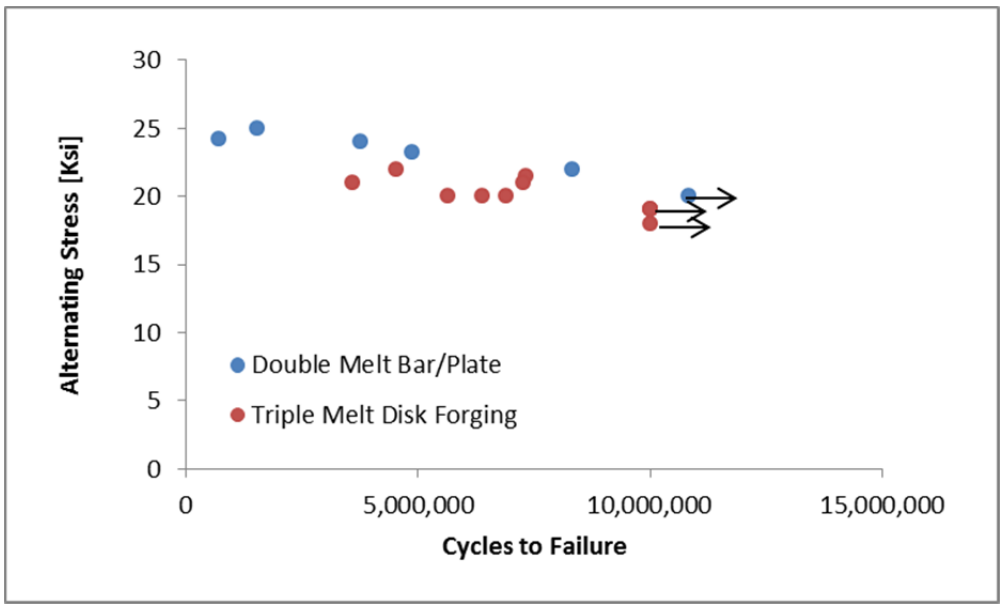

Figure 57: High cycle fatigue data from Haynes®282® disk forging [A= 0.5]

Figure 58 shows the low cycle fatigue behavior of Haynes®282® forging from all orientations, 1400 F, 20 cpm and triangular waveform. All data is compared to commercially available Haynes®282® [Phase 1 report]. The benefits obtained in the fatigue life due to the finer grain, is evident from the figure.

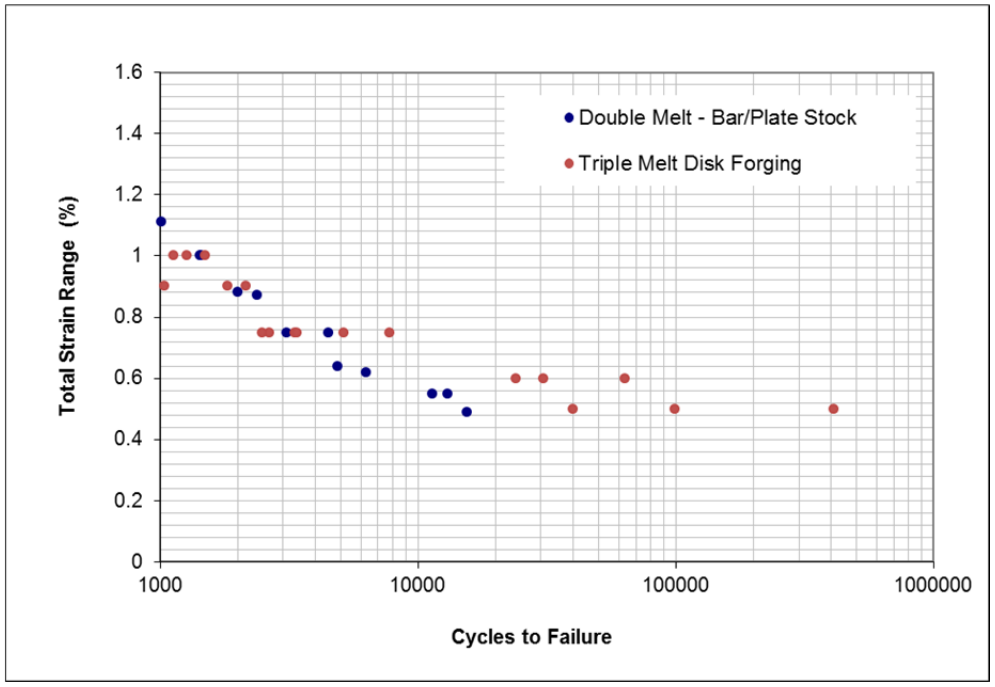

Figure 58: Low cycle fatigue data from Haynes®282® disk forging compared to commercially available Haynes®282® billet/bar

Hold time fatigue tests were performed from the large disk forging similar to the commercially available Haynes®282® billet/bar form [Figure 30]. All hold time fatigue tests were performed at 1400°F (760°) with a trapezoid waveform with a 6 hour and 1 hour hold at peak strain. Figure 59 compares the life obtained and compared to low cycle fatigue in the absence of hold time [Figure 58]. The debit in the hold time fatigue behavior was reduced dramatically by the refined structure.

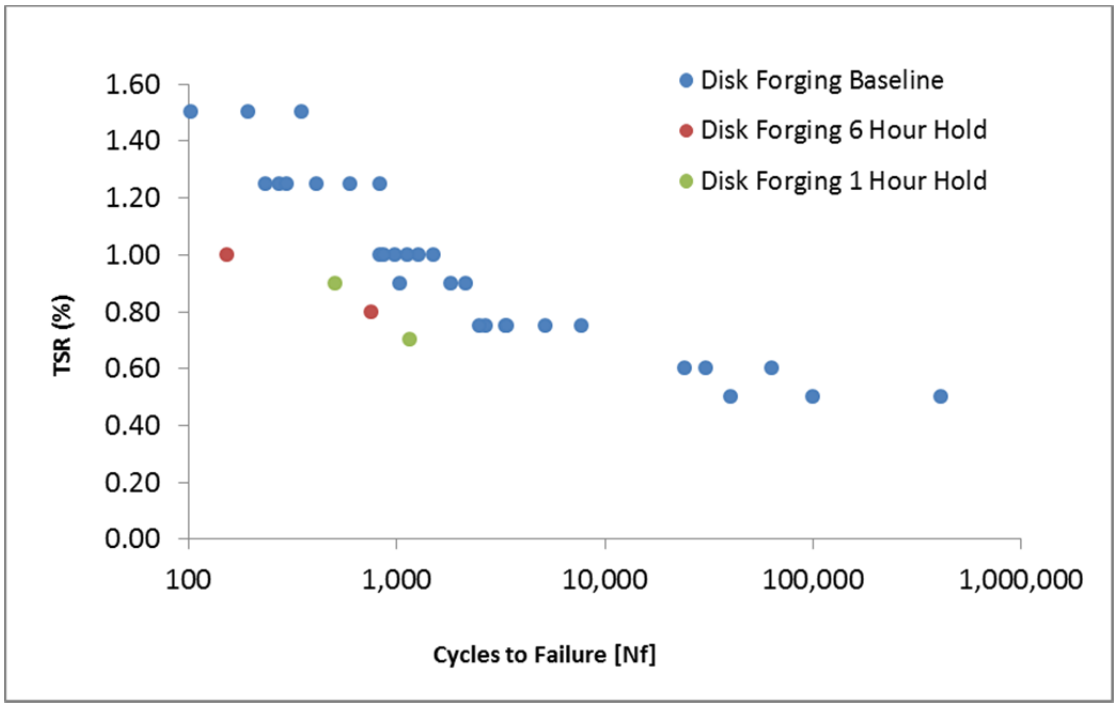

Figure 59: Hold Time Haynes®282® disk forging.

Multiple specimens were extracted from the forging for fracture toughness testing. The specimens were 0.75" thick [B] & 1.5" wide [W]. All specimens were side grooved to a depth equal to 20% of the nominal thickness [10% each side]. The specimens were tested in accordance to ASTM E1820-09. Figure 60 compared the conditional fracture toughness obtained from the fine grained disk to the commercially available Haynes®282® billet/bar. It is also clear from the figure on the gains obtained in the fracture toughness of the alloy due the finer grain size.

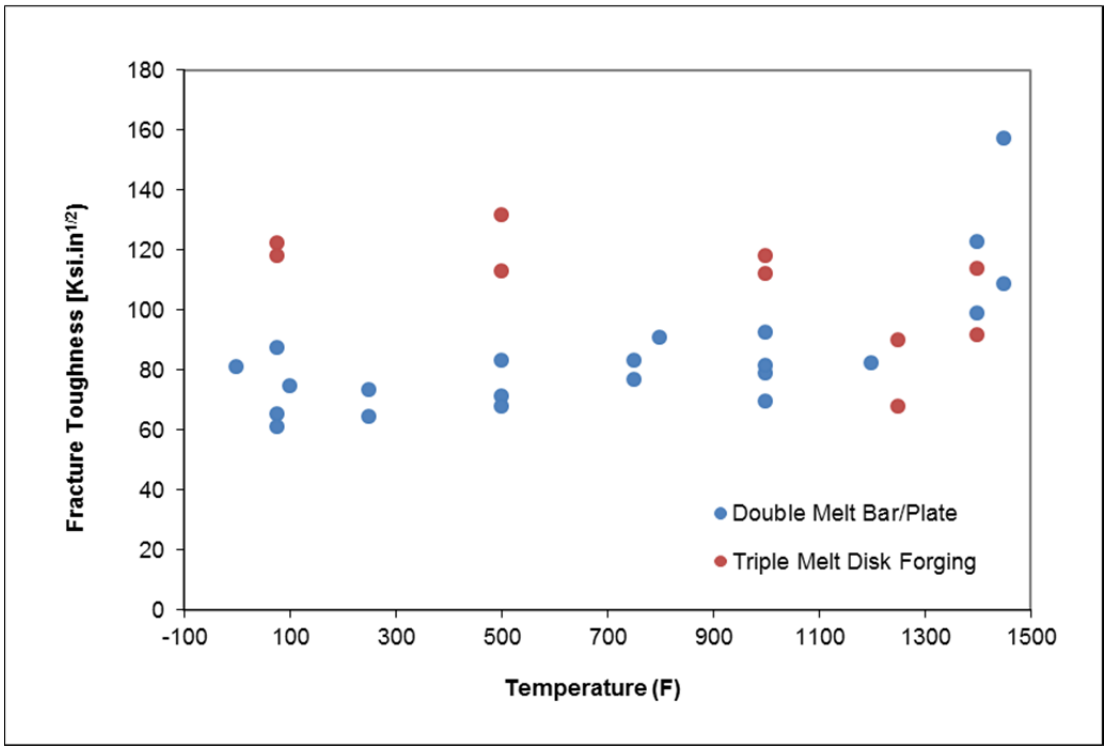

Figure 60: Fracture toughness of Haynes®282® disk forging compared to commercially available Haynes®282® billet/bar

Specimens were extracted for the development of fatigue crack growth rates in the forged Haynes®282®. All tests were performed in accordance to ASTM E647-08, Sinusoidal Waveform and 20 Hertz at room temperature (RT), 1200°F (649°C), 1300°F (704°C) and 1400°F (760°C). Figure 61 shows the curves obtained from the tests. Figure 62 compares the fatigue threshold obtained in the tests as a function of temperature and R ratio.

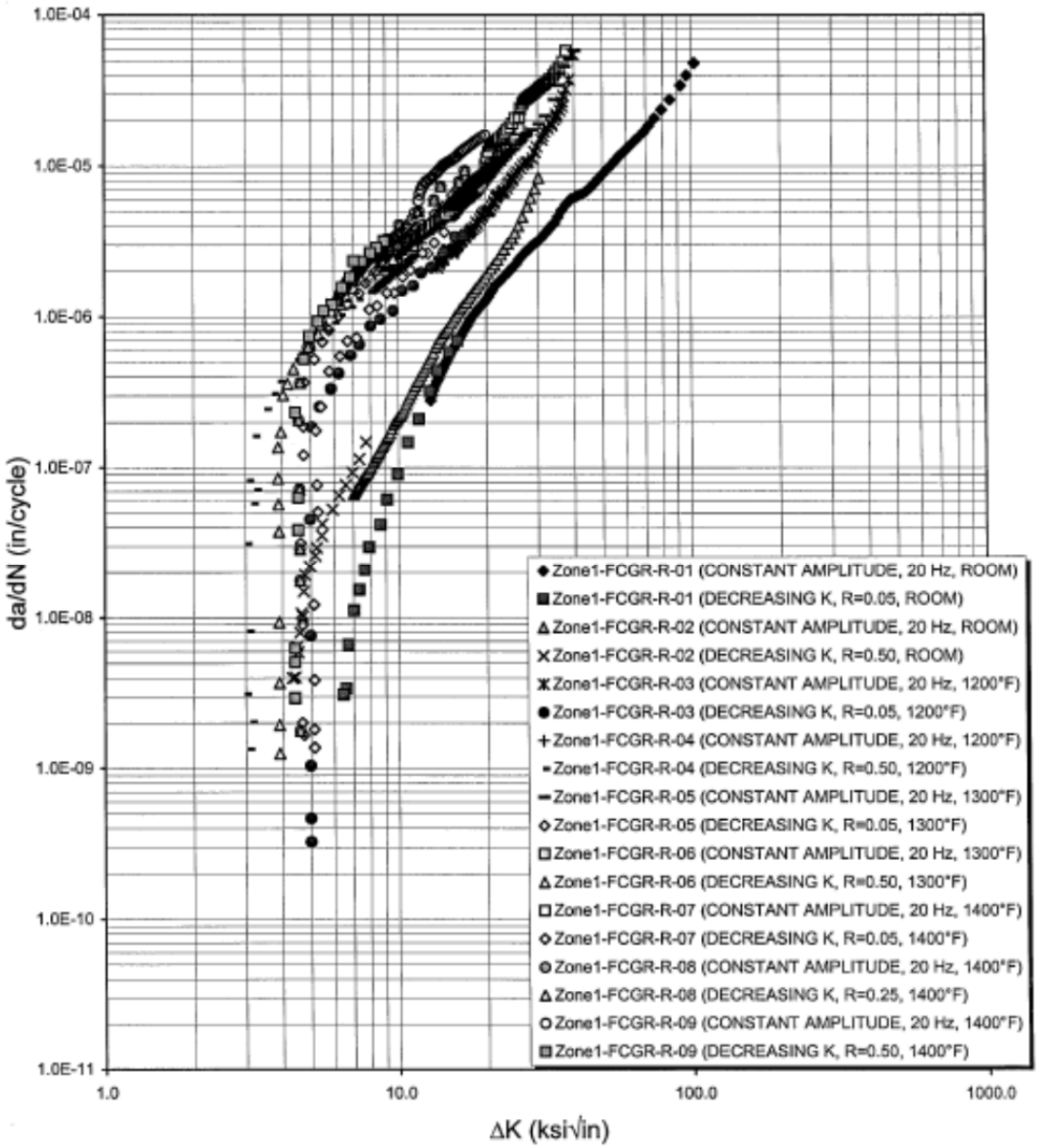

Figure 61: Fatigue crack growth rates in Haynes®282® disk forging

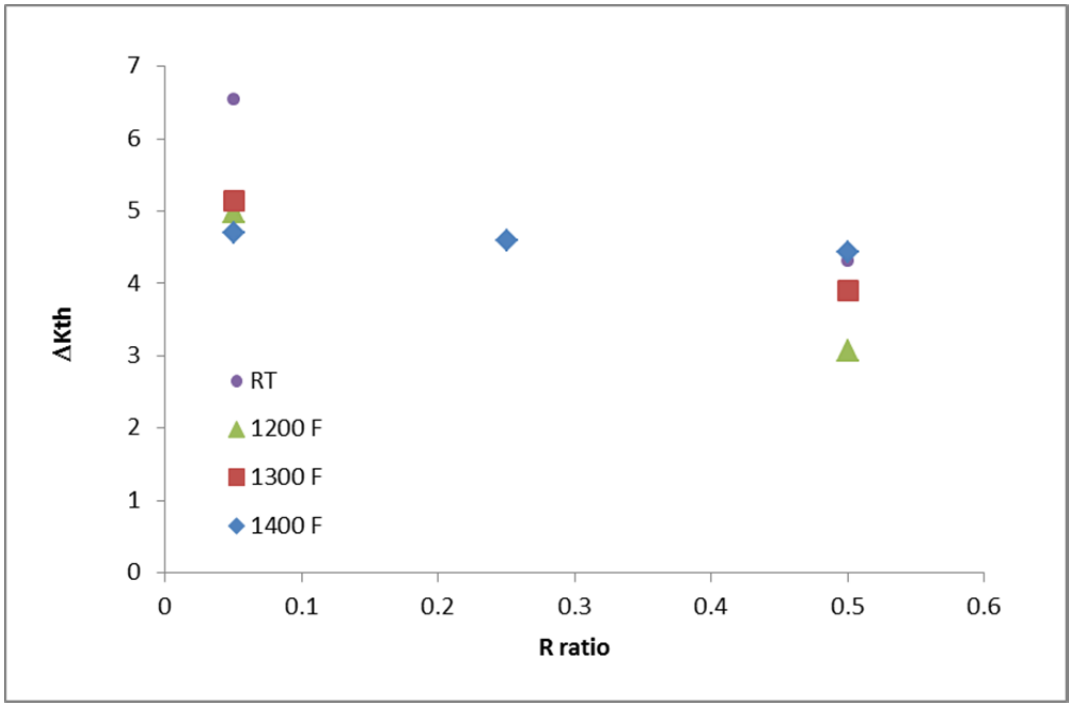

Figure 62: Fatigue threshold in Haynes®282® disk forging as a function of R ratio at various temperatures.

Creep specimens were machined from the disk to evaluate the creep-rupture properties obtained from the forged Haynes®282®disk. Table 3 shows the data obtained from the specimens.

Table 3: Creep-Rupture data obtained from Haynes®282®disk

	Temp	Stress	Time	% Elong.	% RA	% Def.
H282-1	1300	62.5	661	37.8	65.5	27.5
H282-2	1300	55	1307	31.9	63.7	31.6
H282-3	1400	40	477	51.4	79.2	42.9
H282-4	1400	35	872	50.3	76.7	44.4
H282-5	1450	32	264	82.1	83.0	48.5
H282-6	1450	27	590	55.4	79.7	45.6
H282-7	1300	50	2593	43.5	72.6	38.7
H282-10	1400	30	2301	44.9	75.1	39.8
H282-11	1400	25	4655	43.9	63.7	40.4
H282-13	1450	20	2752	57.1	70.3	52.4
H282-8	1300	45	4985	40.6	72.7	33.4
H282-9	1300	40	6771	Stopped Prior to Failure		
H282-12	1400	20	6771			
H282-14	1450	15	6771			
H282-15	1450	10	6771			

Figure 63 is a plot obtained from the fine grained Haynes®282® disk compared to commercially available Haynes®282® material. There is a reduction in life due the fine grained material [approximately 1LMP].

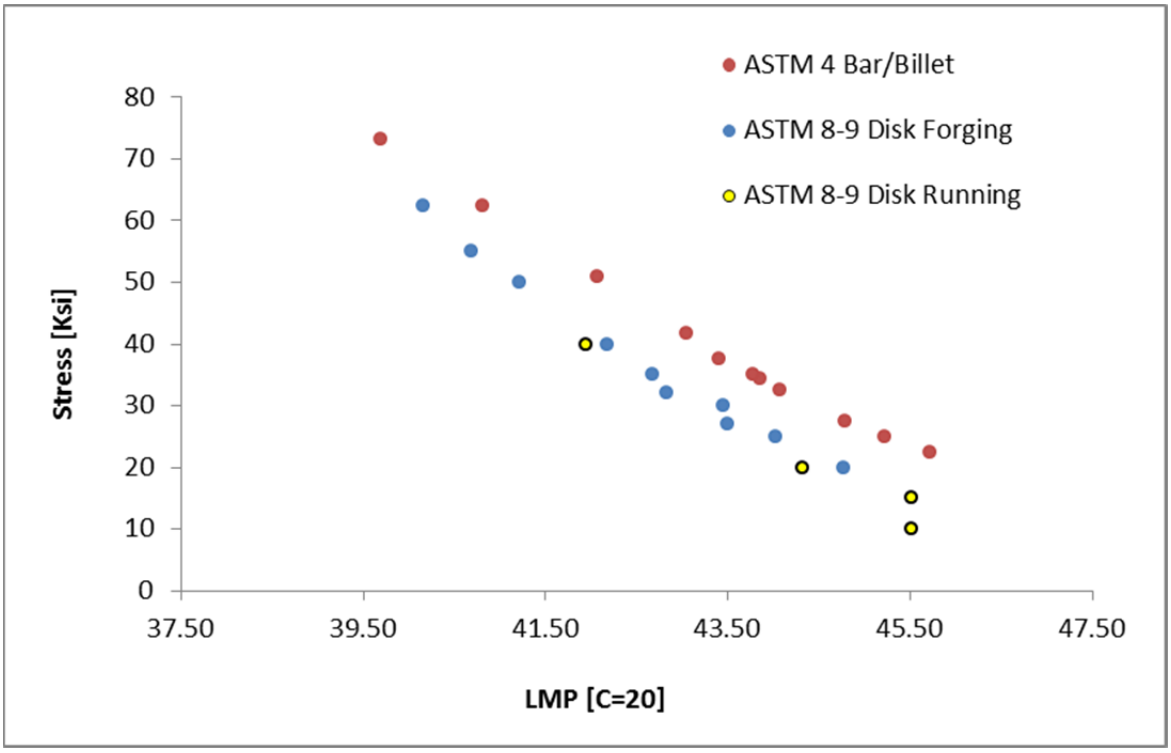

Figure 63: LMP – Rupture Stress plot of Haynes®282® disk forging

The complete dataset from the commercially available Haynes®282® [ASTM 3-4] and the finer grain size disk forging [ASTM 8-9] offer an additional design tradeoff to balance creep and fatigue during the future design process

CONCLUSIONS

Commercially available Nimonic 105 and Haynes®282® were evaluated for microstructural stability by long term thermal exposure studies. Material properties requisite for design such as tensile, creep / rupture, low cycle fatigue, high cycle fatigue, fatigue crack growth rate, hold-time fatigue, fracture toughness, and stress relaxation are documented in this report.

A key requisite for the success of the program was a need demonstrate the successful scale up of the down-selected alloys, to large components. All property evaluations in the past were performed on commercially available bar/billet forms. Components in power plant equipment such as rotors and castings are several orders in magnitude larger and there is a real need to resolve the scalability issue. Nimonic 105 contains high volume fraction γ' [>50%], and hence the alloy is best suited for smaller forging and valve internals, bolts, smaller blades. Larger Nimonic 105 forgings, would precipitate γ' during the surface cooling during forging, leading to surface cracks. The associate costs in forging Nimonic 105 to larger sizes [hotter dies, press requirements], were beyond the scope of this task and not investigated further. Haynes®282® has 20 - 25% volume fraction γ' was a choice for large components, albeit untested.

A larger ingot diameter is pre-requisite for a larger diameter forging and achieves the “typically” accepted working ratio of 2.5-3:1. However, Haynes®282® is manufactured via a double melt process [VIM-ESR] limited by size [<18-16” diameter], which limited the maximum size of the final forging. The report documents the development of a 24” diameter triple melt ingot, surpassing the current available technology. A second triple melt ingot was manufactured and successfully forged into a 44” diameter disk. The successful developments in triple melting process and the large diameter forging of Haynes®282® resolved the scalability issues and involved the first of its kind attempt in the world for this alloy. The complete characterization of Haynes®282® forging was performed and documented in this report. The dataset from the commercially available Haynes®282® [grain size ASTM 3-4] and the finer grain size disk forging [ASTM 8-9] offer an additional design tradeoff to balance creep and fatigue during the future design process.